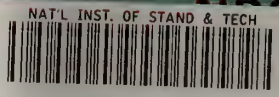


Reference

NBS  
Publi-  
cations

NBSIR 83-2674



A11106 260276

# Color Analysis for the National Bureau of Standards 1016 mm Guarded Hot Plate

---

U.S. DEPARTMENT OF COMMERCE  
National Bureau of Standards  
National Engineering Laboratory  
Center for Building Technology  
Washington, DC 20234

February 1983

Issued April 1983

This work was jointly sponsored by the Department of Energy and the National Bureau of Standards.



---

U.S. DEPARTMENT OF COMMERCE  
NATIONAL BUREAU OF STANDARDS

QC  
100  
.U56  
No. 83-2674  
1983



APR 29 1983

NBSIR 83-2674

**ERROR ANALYSIS FOR THE NATIONAL  
BUREAU OF STANDARDS 1016 mm  
GUARDED HOT PLATE**

---

Brian Rennex

U.S. DEPARTMENT OF COMMERCE  
National Bureau of Standards  
National Engineering Laboratory  
Center for Building Technology  
Washington, DC 20234

February 1983

Issued April 1983

This work was jointly sponsored by the Department of Energy and the National Bureau of Standards.

**U.S. DEPARTMENT OF COMMERCE, Malcolm Baldrige, *Secretary***  
**NATIONAL BUREAU OF STANDARDS, Ernest Ambler, *Director***



## PREFACE

This report is one of a series documenting NBS research and analysis efforts to support the Department of Energy/National Bureau of Standards' Measurements Program. The work reported in this document was performed cooperatively and supported by DoE/NBS Task Order A008 under Interagency Agreement No. DE-AI01-76PRO6010.

#### ABSTRACT

An error analysis is given for the 1-meter Guarded Hot Plate at the National Bureau of Standards. This apparatus is used to measure the thermal resistance of insulation materials. The individual contributions to uncertainty in thermal resistance are discussed in detail. The total uncertainty is estimated to be less than 0.5 percent at sample thicknesses up to 150 mm (6 inches) and less than 1 percent at a thickness of 300 mm (12 inches).

Keywords: apparent thermal conductivity; error analysis; guarded hot plate; thermal insulation; thermal resistance.

## TABLE OF CONTENTS

	<u>Page</u>
ABSTRACT .....	iv
LIST OF FIGURES .....	vi
LIST OF TABLES .....	vi
ACKNOWLEDGMENTS .....	vii
1. INTRODUCTION .....	1
2. PRINCIPLE OF MEASUREMENT .....	2
3. ERROR ANALYSIS .....	3
3.1 SUMMING OF INDIVIDUAL UNCERTAINTIES .....	3
3.2 SUMMARY LIST OF INDIVIDUAL UNCERTAINTIES .....	3
3.3 METER-AREA .....	4
3.4 THICKNESS .....	5
3.5 HEAT FLOW .....	7
3.5.1 $Q_{\text{meter}}$ .....	8
3.5.2 $Q_{\text{resistor}}$ .....	9
3.5.3 $Q_{\text{gap}}$ .....	9
3.5.4 Gap Theory .....	12
3.5.5 $Q_{\text{edge}}$ .....	14
3.6 TEMPERATURE MEASUREMENT .....	16
3.6.1 Overview .....	16
3.6.2 PRT Circuit Rationale .....	16
3.6.3 PRT Calibration .....	16
3.6.4 PRT Self-Heating Uncertainty .....	17
3.6.5 Temperature Distribution Over Meter Area .....	17
3.6.6 Summary of Temperature Uncertainties .....	19
3.7 PLATE EMITTANCE .....	19
4. TOTAL UNCERTAINTY .....	22
5. VERIFICATION OF UNCERTAINTY ESTIMATE .....	24
6. REFERENCES .....	25

LIST OF TABLES

	<u>Page</u>
Table 1. Percentage Estimate of Uncertainties in the Measured Apparent Thermal Conductivity for the NBS Guarded Hot Plate .....	26

LIST OF FIGURES

	<u>Page</u>
Figure 1. Heat flow (Q) in a two-sided guarded hot plate .....	27
Figure 2. Side view of gap .....	28
Figure 3. Plate support and thickness calibration .....	29
Figure 4. Thickness transducer for L-map .....	30
Figure 5. Circuit for meter-area power measurement .....	31
Figure 6. Hot-plate, meter-area power, $Q_m$ , <u>versus</u> gap voltage .....	32
Figure 7. Calculated angular temperature distribution at gap .....	33
Figure 8. Diagram of gap thermopile junctions .....	34
Figure 9. Voltage circuit and wire configuration for the gap thermopile .....	35
Figure 10. The change in apparent thermal conductivity, $\lambda$ , as a function of ambient temperature .....	36
Figure 11. Circuit for the platinum-resistance thermometer (PRT) resistance measurement .....	37
Figure 12. Theoretical plot of the hot-plate, meter-area radial temperature distribution .....	38
Figure 13. Measured hot-plate, meter-area radial temperature distribution .....	39
Figure 14. Figure showing temperature uncertainty due to hot plate PRT location .....	40

## ACKNOWLEDGMENTS

The author expresses his appreciation to Dave Ober, who developed most of the instrumentation and many of the concepts herein, to Rocky Somers and John McAuley for their tireless efforts to improve and run the apparatus, and to Robert Jones and Frank Powell for their leadership in this task.



## 1. INTRODUCTION

This report gives the error analysis of the National Bureau of Standards (NBS) 1016 mm Guarded Hot Plate (GHP) apparatus. It begins with a brief description of the apparatus and of the measured quantities necessary to calculate the thermal transmission properties of a sample material. A method to add the individual uncertainty contributions is rationalized. There follows a detailed discussion of upper-bound estimates of the random and/or systematic uncertainties associated with each measured or modeled parameter. The propagation of errors is accomplished by summing these estimates. There is a discussion of the steady state condition and repeatability. Finally, there is a discussion of how to compare results among different apparatuses, such as would pertain in a round-robin test series. The uncertainties herein apply to the apparatus only, and not to uncertainties associated with material variability of insulation samples.

## 2. PRINCIPLE OF MEASUREMENT

The guarded hot plate measures the heat flow through a sample for a particular temperature boundary condition. Figure 1 shows the basic features of the apparatus in a two-sided configuration with equivalent specimens on either side of the hot plate and with both cold plates at the same temperature. There is a resistance heater in the meter area, A, of the hot plate. The power, Q, produced by this heater is measured. In order to ensure the most accurate and repeatable characterization of a sample, it is necessary that this meter heat flow straight across to the cold plates--that is, that its direction be in one dimension. For this reason, the guard area of the hot plate is maintained at the same temperature as the meter area. Assuming that the metered heat is split evenly between the two sides, the average thermal resistance, R, of the two sides of the sample pair is calculated by

$$R = \frac{\Delta T A}{(Q_m/2)} \quad (1)$$

That is, R is defined in terms of the basic quantities  $Q_m$  and A, and of the boundary conditions, namely the hot plate and the two cold plate temperatures. The term  $\Delta T$  is the average of the temperature differences between the hot plate and the two cold plates. An additional parameter is the specimen thickness, L, averaged over both sides. The apparent thermal conductivity,  $\lambda$ , is defined by

$$\lambda = \frac{L}{R} = \frac{Q_m L}{2A \Delta T} \quad (2)$$

Note that each of the above parameters represents an average over the meter area and over the two sides. The procedure is to place specimens in the apparatus and to monitor the plate temperatures and the power,  $Q_m$ , to establish when these become constant--to within the limits of the instrumentation control. The test is defined to be in steady state when subsequent values of R (or  $\lambda$ ) vary randomly about the mean value. Typically, the R-value can be controlled within a few hundreds of a percent, and when the R-value does not change by more than this amount within ~5 hours there is good confidence that steady state has been achieved. The time required to achieve steady state varies from ~2 hours for a 75 mm-thick, 10 kg/m<sup>3</sup> sample to ~30 hours for a 300 mm-thick, 130 kg/m<sup>3</sup> sample. Finally, the apparatus can test a sample on only one side of the hot plate (referred to as a one-sided configuration) by maintaining the temperature of the other cold plate approximately equal to the temperature of the hot plate.

### 3. ERROR ANALYSIS

#### 3.1 SUMMING OF INDIVIDUAL UNCERTAINTIES

The apparent thermal conductivity and the thermal resistance of an insulation sample are calculated quantities based on several measured parameters. Each of these measured parameters has an uncertainty. In turn, this uncertainty has a random and systematic (or constant) part. It is possible to estimate the uncertainty of each parameter by an independent test. For example, the apparatus thickness readout can be compared with an independent thickness detector placed between the plates. This independent detector offers the advantages that it is more precise and more easily calibrated and it can be located in the region of actual interest.

It is not straightforward to estimate the overall uncertainty of the calculated quantity, because there is usually not sufficient information on the breakdown between the random and systematic parts for each individual parameter. In principle, it is possible to gather this information, but in practice it would be too time consuming.

A simple and practical approach was used in this error analysis. The individual parameters, such as the thickness or temperature distribution over the meter area, were measured with an independent detector under test temperature conditions. A comparison of the apparatus readout with these independent measured values made possible the estimate of an upper bound on the total uncertainty for each parameter. Since there is not sufficient information to assure that the measured values are randomly distributed about a "true" mean value, the upper bounds for each individual parameter are simply added to arrive at the overall uncertainty. This is different from an alternative approach to treat the uncertainties as standard deviations with the total uncertainty being calculated as the square root of the sum of the squares of the individual standard deviations. This "upper bound" approach results in a somewhat larger estimate of the overall uncertainty (by as much as 30 percent), but it avoids the need to make an inordinate number of check-up measurements to assure that there are no outlier values. This more conservative approach is thought by the author to be appropriate for a national insulation standards lab.

The following philosophy was used with regard to the estimate of upper bounds. Even if an uncertainty might have been expected to be smaller, based on theoretical considerations and manufacturer specifications, the uncertainty value actually used was that of the detector making the independent check. For example, the plate temperature might very well be known within 5 or 10 mK. The uncertainty value actually used, of 22 mK, was associated with the thermopile used to independently check the uniformity of the plate temperature. That is, the claim did not go further than what could be empirically demonstrated.

#### 3.2 SUMMARY LIST OF INDIVIDUAL UNCERTAINTIES

The following is a list of measured parameters that contribute to the major individual uncertainties which will be discussed in detail in the next sections: meter area, sample thickness, meter-area heat flow, heat flow across gap

between the guard and meter areas, net heat flow to the sample edge, and plate temperatures.

### 3.3 METER-AREA

The value of the circular meter area, A, in equation (2) corresponds to the radius at the geometric center of the gap (refer to figure 2). Since the measured values are 0.20282 m (7.985 inches) for the inner radius,  $r_1$ , and 0.20371 m (8.020 inches) for the outer radius,  $r_o$ , then the geometric-center radius,  $r_c$ , is calculated as follows:

$$r_c = \left( \frac{r_o^2 + r_1^2}{2} \right)^{1/2} \quad (3)$$

$$r_c = 0.20326 \text{ m (8.0025 in)}$$

The systematic error in  $r_c$  was estimated to be not more than 0.012 mm [0.0005 inches]. This was the machining uncertainty estimate.

This radius corresponds to a temperature of 295.2K [72°F]. When the hot plate is at another temperature, the thermal expansion of the plates must be considered. The radius corresponding to the meter area is calculated by

$$r'_c = r_c(1 + \alpha(T_h - 295.2K)) \quad (4)$$

Typically,  $T_h = 310.8 \pm 1 \text{ K (100 F } \pm 2 \text{ F)}$ .

$\alpha$  = the coefficient of thermal expansion for the Aluminum hot plate (type 6061-T6).

$$\alpha = (24.3 \pm 1) \times 10^{-6} \text{ m/m}\cdot\text{K}$$

The meter area is calculated by

$$A = \pi r_c'^2 \quad (5)$$

The set of independent variables for A is  $\{r_c, T_h, \alpha\}$ . The values of the uncertainties in these variables,  $\Delta_i$ , are as follows:

$$\Delta_r = 0.012 \text{ mm}$$

$$\Delta_T = 1 \text{ K}$$

$$\Delta_\alpha = 4 \times 10^{-6} \text{ m/m K}$$

The contributions from the  $\Delta_T$  and the  $\Delta_\alpha$  terms are negligible, so the present uncertainty in A is

$$\frac{\Delta_A}{A} \approx \frac{2\Delta_r}{r_c} = .0001 = .01 \text{ percent} \quad (6)$$

$$\begin{aligned}
 A(37K) &= \pi r_c'^2 & (7) \\
 &= 0.12990 \text{ m}^2 \pm 0.000016 \text{ m}^2 \\
 &= 201.3397 \text{ in}^2
 \end{aligned}$$

Note, this meter area corresponds to the sample area through which the heat generated in the meter area heater would flow if the heat flow were one-dimensional.

### 3.4 THICKNESS

The parameter L in equation (2) refers to the average specimen thickness over the meter area. For low-density or compressible specimens this is best estimated by the value of the average plate spacing over the meter area. Precaution should be taken to compress such a sample slightly, so as to avoid voids between the specimen and the plates. For rigid specimens, there are two possible ways to estimate the test thickness. First, if the specimen surfaces and the plates are sufficiently flat and parallel, then the plate spacing is a good estimate. Second, if any of these surfaces are irregular, then the specimen thickness itself should be measured--with a caliper, for example. There should then be an estimate of the thermal resistance of the small air gaps at the irregular surfaces. This should be negligible.

The measurement of the plate spacing is described below. The basic calibration method is to measure the positions of the four outside "corners" of the cold plates relative to a known meter-area plate separation. These outside cold-plate positions are measured using four thickness transducers on each plate. Then these thickness transducers measure any change in position relative to the initial calibration point. This calibration must be done for each plate orientation and for compressible and rigid samples.

The following is a more detailed discussion of the thickness calibration--referred to as the L-map. Please refer to figure 3. Here is shown the basic plate support and measurement system. The hot plate is rigidly and permanently mounted on the four support rods. The cold plates are supported in the center. This point of support has a load cell to measure the force that the sample exerts on the plate. It also has a ball joint so that the plate can tilt to conform to a nonparallel rigid sample. The cold plates are constrained in the radial direction by steel cables attached to four spring loaded bearings which are mounted on stainless-steel rods with a diameter of 51 mm (2 inches).

At four points (at 90° intervals) at the edge of each cold plate the positions (perpendicular to the plates) are measured with thickness transducers (referred to as Ftt). The manufacturer's stated overall accuracy over a displacement of 150 mm (6 inches) is within 10 μm (0.0004 inches) for a single Ftt. The mean displacement of the four Ftt's on a single cold plate would then be known within a factor of 1/√4 or 5 μm (0.0002 inches). The Ftt's are mounted on Invar bars to minimize error due to temperature variation of the ambient. A coefficient of thermal expansion value of 10<sup>-6</sup>m/m·K, a length of .25 m (10 inches) and a temperature range of 50 K correspond to a length change (or

error) of  $13\ \mu\text{m}$  (0.5 mil). This contribution to error is avoided by the calibration procedure to be described later, since it is performed at the ambient temperature appropriate to the test.

The calibration procedure is to correlate an absolute measurement of the average meter area spacings with average displacements of the Ftt's. The Ftt's will then provide any displacements from this original calibration point, provided the plates remain in the same orientation--that is, that they are not rotated. The absolute measurement of the average meter area spacing is made with thickness transducers such as that shown in figure 4. This measurement is made with the plates both horizontal and vertical, since the plate sag is different in the two cases. These thickness transducers were calibrated with an uncertainty of 5 micrometers ( $\mu\text{m}$ ), (0.2 milli-inches or mils), using NBS gauge blocks accurate within  $0.3\ \mu\text{m}$  (0.01 mils) at 293.15 K (20 C). The uncertainty in the gauge block length, due to temperature difference from that of calibration when the gauge block was calibrated, is estimated to be  $3\ \mu\text{m}$  (0.1 mils). The measured flatness within the meter area is  $\pm 25\ \mu\text{m}$  (1 mil). In the L-map, the plate spacing is measured at 25 points in the meter area. The repeatability of the average of these 25 points was  $5\ \mu\text{m}$  (0.2 mils). Thus the uncertainty is about  $1/5 = 1/\sqrt{25}$  times the flatness.

The next step is to measure the difference between the spacing at the center of the meter area and the average spacing over the meter area (the average of the 25 points). The reason is that the calibration procedure can then rely on the measurement at one point at the center, rather than require 25 points. Another  $2.5\ \mu\text{m}$  (0.1 mil) value is added due to the transducer uncertainty for the transducer center point measurement.

To understand the final contribution to thickness uncertainty we must look at the problem of plate bowing deformation. The plates are 1 m (40 inches) in diameter. The cold plates are 19 mm (0.75 inches) thick and weigh about 50 kg (110 lb). The hot plate is 16.13 mm (0.635 inches) thick and weighs about 32 kg (70 lb). Referring to figure 3, the various forces that act to deform the plate are due to the load cell at the center, the weight of the plates and the spring-loaded cables at the four corners. As the cold plates open and close, they tilt, which causes a deformation change. The problem with the bowing deformation is the following. The Ftt readings correspond to four thickness points at the plate edges, and the average of these is not necessarily the same as the value at the plate center, when there is a bowing deformation. Repeatability studies compared the Ftt thickness values with those of a transducer at the plate center, after the cold plates have been opened and closed back to the original thickness. These gave a repeatability of  $5\ \mu\text{m}$  (0.2 mils). Note that it is important that the stainless steel plate support rods be straight and parallel to have the best repeatability.

To review, the calibration procedure uses thickness transducers which are calibrated with NBS gauge blocks and placed in the center of the meter area, between the hot and cold plate, at the test thickness and temperature. The transducer reading then is used to set the 8 Ftt's (4 on each side). The plates are then opened, the samples are put in and the plates are closed to the

test condition. Below is a summary of the uncertainties,  $\Delta_1$ , that contribute to the thickness uncertainty for compressible (low-density) specimens.

	$\Delta_1$	$\mu\text{m}$	mil
auxiliary thickness transducer		5	0.2
thermal expansion of gauge block		2.5	0.1
$\Delta$ between average and center meter-area spacing		5	0.2
$\Delta$ of center position		2.5	0.1
$F_{tt}$ (Farrand transducer)		5	0.2
<u>repeatability after opening and closing cold plates</u>		<u>5</u>	<u>0.2</u>
total = $\Delta_1$		25	1.0

### 3.5 HEAT FLOW

There are a number of heat flows, designated by  $Q$ , involved in the guarded hot plate apparatus (refer to figure 1). There is the heat generated by the meter heater,  $Q_m$ , and the heat generated by any resistive sensors in the meter area,  $Q_r$ . There is the heat flow between the meter area and the guard area,  $Q_g$ , which consists of a part flowing directly across the gap,  $Q_o$ , and a part flowing through the specimen,  $c\lambda$ . Here,  $\lambda$  is the thermal conductivity of the specimen. Also, there is some net heat flow between the meter area and the ambient through the specimen. This will cause the actual heat flow leaving the meter area to be different from the idealized one-dimensional heat flow. The difference is the edge heat flow,  $Q_{ed}$ .  $Q_{ed}$  depends on the guard and meter widths, on the thickness, on the ambient and plate temperatures and on the sample  $\lambda$ -value. The final, "apparatus-independent", meter-area heat flow must take into account these correction terms.

Even then, it is not entirely apparatus-independent, even in principle, because part of the heat flow is by radiation. This means that the heat flow across the sample depends on the plate emittance,  $\epsilon$ . Intuitively this can be understood since a smaller emission of thermal radiation from the plates will result in a smaller sample heat flow. The easiest way to minimize this apparatus dependence is to standardize the values of the plate emittances. The ASTM Test Method 177 for the guarded hot plate requires that this emittance value be approximately 0.90. This standardization is intended to minimize discrepancies among the various apparatuses. Then, if an apparatus has a different emittance value or an uncertainty in emittance value, the adjustment or uncertainty in the measured  $\lambda$  could be calculated. This is discussed in more detail under the section on plate emittance.

### 3.5.1 $Q_m$ meter

Let us now look at each heat-flow term in more detail. The first term,  $Q_m$ , is the power produced by the meter heater. Figure 5 shows the schematic for for this measurement. A known standard shunt resistor,  $R_s$ , of approximately  $0.1 \Omega$ , that is maintained in an oil bath, is used to determine the current. Voltage taps across the meter heater lead wires in the center of the gap are used to measure the voltage corresponding to the power that would be expected to travel one-dimensionally to the cold plate.

$$Q_m = \frac{V_{\text{heater}} V_s}{R_s} \quad (8)$$

The value of  $R_s$  is calibrated at one year intervals.

$$R_s = 0.1000700 \Omega \pm 5 \text{ ppm at } 25.0^\circ\text{C}$$

An additional uncertainty of 20 ppm is included since the resistor is in a bath at  $28^\circ\text{C}$ . The uncertainty of 25 ppm corresponds to a 0.0025 percent uncertainty, which is negligible compared with other uncertainties.

If the heater voltage taps were not in the center of the gap, there would be an error in the measurement of  $V_{\text{heater}}$ . The nichrome wire size is 28 gauge which has a resistance value of  $42 \Omega/305 \text{ m}$  (1000 ft). Assuming (conservatively) that the taps might be misplaced by half the gap width of 6 mm (0.23 in), then the error in  $R_{\text{heater}}$  is calculated to be  $8 \times 10^{-4} \Omega$ . This is negligible when compared with the value of  $R_{\text{heater}}$  of approximately  $56 \Omega$ . Next we need to consider the accuracy of the voltage measurements. The heater voltage,  $V_{\text{heater}}$ , varies from about 8 volts to 27 volts for one- and two-sided operation at thicknesses of 25 to 150 mm (1 to 6 inches). The shunt voltage  $V_s$  varies from about 14 mV to 48 mV for the same range of operation. The following equations are needed to calculate the the uncertainties. First, in order to calculate the approximate  $Q_m$  for a particular specimen in the two-sided mode we use

$$Q_m = \frac{2 \lambda \Delta T A}{L} \quad (9)$$

For low-density material,  $\lambda \approx 0.046 \text{ W/m}\cdot\text{K}$

$A \approx 0.1299 \text{ m}^2$ , and  $\Delta T = 27.8 \text{ K}$ . For  $L \approx 150 \text{ mm}$ ,  $Q_m \approx 2 \text{ W}$ .

Also  $R_{\text{heater}} \approx 56 \Omega$  and  $R_s \approx 0.1 \Omega$ .

Thus  $V_{\text{heater}} \approx 560 V_s$

Once  $Q_m$  is known, we can calculate  $V_s$  with equation (8).

$$V_s = \left( \frac{R_s Q_m}{560 \Omega} \right)^{1/2} \approx 20 \text{ mV for the previous example}$$

Thus  $V_{\text{heater}} \approx 10 \text{ V}$ .

These order-of-magnitude estimates are necessary to calculate the percentage errors in  $V_{\text{heater}}$  and  $V_S$ . As an example, for the 10 V range and for a 90 day period, the manufacturer's specifications give the following formula to calculate the voltage uncertainty,  $\Delta v$ .

$$3 \Delta v = \frac{(0.0023)}{100} V + 2 \text{ counts} \times \text{count value} \quad (11)$$

This is for a 6 digit readout and an average over 10 power line cycles. The count value is somewhat larger than the minimum detectable signal and has a value of 10  $\mu\text{V}$ . If  $V = 8\text{V}$ ,  $\Delta v = .000008 = .0008$  percent. This is obviously negligible compared to other voltage errors. Another example is the reading of  $V_S$  on the 0.1 V scale. Let  $V_S = 14 \text{ mV}$ , which is a worst-case value.

$$\begin{aligned} 3 \Delta v &= \frac{(0.0034)}{100} \times 20 \text{ mV} + 24 \text{ counts} \times 0.1 \mu\text{V} \\ &= 3.1 \mu\text{V} \\ \frac{3 \Delta v}{V_S} &= 0.00015 = 0.015\% \end{aligned} \quad (12)$$

This  $\Delta v$  uncertainty is the only contributor to the uncertainty in  $Q_m$  that is not negligible, and it is mostly due to the "24 counts". We will use a worst-case value of 0.04 percent for  $\Delta Q_m/Q_m$ .

### 3.5.2 $Q_{\text{resistor}}$

The resistive devices in the meter area generate a small amount of power,  $Q_R$ , which must be added to  $Q_m$ . These devices include a platinum resistance thermometer, RTD for plate temperature readout and two thermistors,  $R_{\text{th}}$ , one for hot plate control and one for the control of heat across the gap.

$$R_{\text{RTD}} \approx 100 \Omega; I = 1 \text{ ma}; \text{ thus, } Q_{R1} = 0.1 \text{ mW}$$

$$R_{\text{th}} \approx 1 \text{ K } \Omega; I = 1 \text{ ma}; Q_{R2} = 1 \text{ mW}$$

$$Q_R = Q_{R1} + 2Q_{R2} = 2.1 \text{ mW.}$$

Assuming that  $Q_R$  is known within 20 percent (a conservative estimate),  $\Delta Q_R/Q_m \approx .02$  percent when  $Q_m = 2\text{W}$ .

### 3.5.3 $Q_{\text{gap}}$

A crucial point in the design of a guarded hot plate (GHP) is to minimize the uncertainty due to the heat flow across the gap between the meter and guard areas in the hot plate. The most straightforward method to estimate this error is an empirical one. This method for the NBS-GHP will be discussed first, and a theoretical discussion will be given later.

Looking at the empirical method in more detail, remember that the gap temperature difference is estimated by a thermopile across the gap. In the NBS GHP this is an 18-stage thermopile. In principle, a zero gap voltage would correspond to a zero average temperature difference across the gap, which would, in turn, correspond to a zero net heat flow, across the gap.

The gap is unbalanced by making the average temperature on the meter side of the gap different from the average "guard-side" temperature. This results in a radial temperature gradient at the gap, which gives a non-zero thermopile voltage value for the gap voltage. Since the gap voltage is normally known or maintained to within several  $\mu\text{V}$  of zero, then a reasonable unbalance range might be 30  $\mu\text{V}$ . The slope of the curve showing the change in  $Q$  versus the gap voltage is a measure of the sensitivity of the gap thermopile (see figure 6). Values at a larger unbalance provide a better knowledge of the slope, although points should be taken over the whole range to confirm that the curve is indeed linear at zero  $V_g$ .

The gap sensitivity will be different for various values of specimen thickness and thermal conductivity. Therefore, sensitivity studies must be performed for the entire ranges of these specimen parameters. The values with the 18-stage thermopile of the gap sensitivity for the low-density mineral-fiber insulation material used for the NBS calibration transfer specimens are 0.00056, 0.00057 and 0.00058  $\text{W}/\mu\text{V}$  for  $L = 25, 75, \text{ and } 150$  mm (1, 3, and 6 inches), respectively. The thermocouples comprising the gap thermopile were Chromel-Constantan, Type E, which have a sensitivity of 62.03  $\mu\text{V}/\text{K}$ . Since there are 18 stages, the actual sensitivity is  $18 \times 62.03 = 1116$   $\mu\text{V}/\text{K}$ . The gap sensitivity can be expressed as 0.636  $\text{W}/\text{K}$ . As an example, a  $T_g$  (temperature difference between guard and meter side of gap) value of 0.01  $\text{K}$  would result in a  $Q_g$  value of roughly 6 mW.

The contributions to the uncertainty resulting from the various estimates of the gap voltage are as follows. The first question is how well does a zero gap voltage correspond to a zero heat flow across the gap. The question arises because there is expected to be some angular temperature difference at the gap due to heater and sensor lead wires and the support pins. (These pins bridge the gap to support the meter-area part of the hot plate.) The next question is how accurately can this  $T_g$  (or the corresponding gap voltage,  $V_g$ ) be measured. This depends on the accuracy of the readout device and on the extent to which thermals in the lead wires can be eliminated.

Addressing the first question, a calculation of the angular gap temperature distribution due to heat generated by the heater leads as they come in from the side was performed in reference [3]. Figure 7 shows the results of this calculation for the NBS GHP. For a worst case of a two-sided, low-density mineral fiber sample at one inch thickness,  $Q_m$  would be roughly 12 W, so  $Q_o$  would be about 90  $\text{W}/\text{m}^2$  ( $A = 0.1299 \text{ m}^2$ ). In this case, the maximum temperature difference on the meter side is about 2 mK. (Note that this calculation assumes a zero gap temperature difference, and that there is no insulation around the incoming heater leads. In fact, there is wire insulation, and the plates will be more isothermal than what the calculation shows.)

In fact, the temperature difference is much larger than 2 mK for the following interesting reason. The gap has a thermal conductivity roughly equal to that of air. The thermal conductivity of the aluminum plate is roughly 6000 times greater than that of air. The heat flow is proportional to the product of the thermal conductivity and the temperature gradient. Assuming steady state, then the radial heat flow at the gap (thru the plate and then thru the gap) is constant. This means that the temperature gradient in the gap is 6000 times greater than that in the plate. This means that a radial temperature gradient of 0.2 mK/cm in the plate would give a temperature difference of roughly 100 mK across the gap (the gap width is ~0.9 mm). In effect, the gap acts as an amplifier of the temperature gradient. As far as the heat flow across the gap is concerned, however, this effect is very small.

An experimental study was made to measure the temperature difference across the gap. It used a 16-stage thermopile which was firmly pressed against the plate by a rigid specimen. Temperature differences of the order of 100 mK were measured at positions around the gap, even when the gap voltage indicated an average temperature difference of <1 mK. This study showed that heat flowed into and out of the meter area at various positions around the gap perimeter. Thus, the net gap heat flow should be zero, even when temperature differences ~ 100 mK are measured at points on the gap perimeter.

It would be impossible to make a realistic calculation of the angular distribution of the temperature difference across the gap, because of the aforementioned amplification of temperature difference across the gap and because the plate gradients that are being amplified are so small. Fortunately, it is possible to ascertain empirically that the net gap heat flow is zero.

If one could calculate the gap heat flow as a function of angular position, it would resemble a sinusoidal curve with positive peaks and negative valleys. The danger, as far as error goes, would be that the thermocouple stages of the gap thermopile might all lie on peaks. This would result in a systematic error in the monitored heat flow. Certainly, this unfortunate possibility is less likely if there is a larger number of evenly spaced thermocouple junctions. (Note that the adjacent junctions need not be opposite each other, so the leads can be longer than the gap width.)

A series of calculations was performed on curves of the kind shown in figure 7, to estimate the uncertainty in the knowledge of the mean as function of the number  $N$  of thermocouple stages around the gap. (Let us assume, for the moment, that the temperature difference,  $\Delta T_1$ , is measured exactly.) This study showed that the uncertainty of the mean due to the finiteness of the sampling becomes negligible after  $N$  equals 10. The conclusion, then, is that the angular distribution of gap temperature difference is not constant, but this does not result in any measurable gap error as long as more than 10 thermocouple stages are used.

Another reason to have a large number  $N$  is that the gap voltage increases proportional to  $N$ . Thus the percent uncertainty due to the gap voltage readout resolution decreases proportional to  $1/N$ . This is true as long as the amount of heat transferred across the gap through the thermopile wires is small

compared to the heat flow through the air. For the NBS GHP, this ratio is less than 1/1000 for a single wire. As a note to the experimentalist, it is important to thermally anchor the thermocouple wire (for ~5 mm) before it leaves the plate surface. Also the adjacent thermocouples are staggered to permit the wire crossing the gap to be long (~10 cm) (see figure 8). This is done since the heat flow through the wire is inversely proportional to its length. Next we shall consider the readout error of the gap thermopile. Figure 9 shows a graphical representation of the gap measurement situation. As long as it is a null measurement with the meter, gap and guard temperatures at the same value, there is no readout error in the thermopile signal up to point A.

At point A the 0.25 mm (10 mil) Chromel wire is soldered to the 0.25 mm (10 mil) copper wire, which is very pure and, hence, should have a very small thermal signal ( $\sim 0.1 \mu\text{V}$ ) coming out through the guard. The order of magnitude of the spurious thermal signal due to a temperature difference between the last Chromel-Constantan junction and the Chromel-Copper junction can be estimated as follows. The two Cr-Cu junctions are located in the same location on the guard side of the gap, so an overestimate of the temperature difference between their locations would be 1 mK. The Cr-Cu sensitivity is  $\sim 20 \mu\text{V/K}$ . Thus the spurious signal would be about  $0.01 \mu\text{V}$ , and this is negligible.

The next error source is the thermals generated in the pure copper wire between points A and B in figure 9. If the wire is handled with care and low-thermal solder is used, these thermals should be less than  $0.1 \mu\text{V}$ , and is referred to as  $\Delta V_{\text{AB}}$ . We use a value of  $0.2 \mu\text{V}$  for  $\Delta V_{\text{AB}}$ . (If the Cu wires are connected at A, the actual thermal signal can be measured within the accuracy of the readout device.)

The next error results from any thermal emf's in the reversing switch B or between B and C. The latter error can be eliminated by reversing the signal at B. Any residual thermal signal in the reversing switch can be measured by shorting a copper wire across the switch. This quantity,  $\Delta V_{\text{switch}}$ , is estimated at  $0.2 \mu\text{V}$ . Finally, there is the readout error of the Digital Linear Amplifier,  $\Delta V_{\text{DLA}}$ . This is estimated to be about  $0.1 \mu\text{V}$ . The sum of  $\Delta V_{\text{DLA}}$ ,  $\Delta V_{\text{switch}}$  and  $\Delta V_{\text{AB}}$  is  $0.5 \mu\text{V}$  and this is referred to as  $\Delta V_g$ . Remember that the other contributions to error were estimated to be negligible.

The resulting heat flow uncertainty,  $\Delta Q_g$  is calculated by  $\Delta Q_g = S_g \Delta V_g$ , where  $S_g$  is the gap sensitivity previously discussed. The term  $S_g$  is equal to the slope of the curve of the change in heat flow,  $Q_g$ , as the gap thermopile voltage is unbalanced by an amount equal to  $V_g$ .  $S_g = Q_g/V_g$ . Strictly speaking, this could be a function of  $V_g$ .

The quantity  $S_g$  has a value of  $0.57 \text{ mW}/\mu\text{V}$ , so  $\Delta Q_g$  is estimated to be  $0.3 \text{ mW}$ . The percent uncertainty due to the gap is calculated as the ratio,  $\Delta Q_g/Q_m$ . In the two-sided configuration,  $Q_m \sim 1\text{W}$  at 300 mm (12 in), for low-density insulation samples. The corresponding percentage uncertainty value is  $\sim 0.03$  percent.

#### 3.5.4 Gap Theory

It is possible to model the gap unbalance results with an equation derived by Woodside [2].

$$Q_g = (q_0 + c\lambda)T_g \quad (13)$$

Here  $Q_g$  is the heat flow between the meter and the guard sections of the hot plate as a result of an unbalance in the corresponding temperatures of  $T_g$ . The term  $q_0$  represents the heat flow per unit temperature that flows directly across the gap, and the term " $c\lambda$ " represents the heat flow/unit temperature in the specimen across the boundary between the part of the specimen next to the meter area and the part next to the guard area. Here,  $\lambda$  is the specimen apparent thermal conductivity. Just as  $S_g$  is the heat flow sensitivity per unit voltage,  $S'_g$  is defined as the heat flow sensitivity per unit of temperature difference.

$$Q_g = S_g V_g = S_g S_{tc} T_g \quad (14)$$

$$\begin{aligned} S_{tc} &= \text{the thermopile sensitivity} \\ &= \text{number of stages} \times 62 \text{ } \mu\text{V/K} \\ &= 18 \times 62 \text{ } \mu\text{V/K} \\ &= 1116 \text{ } \mu\text{V/K} \end{aligned}$$

$$\text{Note that } S_g S_{tc} = q_0 + c\lambda.$$

The quantity  $c$  is a constant which depends on the apparatus dimensions and the specimen thickness [2].

$$c \approx \frac{P}{72\pi} \ln(4a), \quad a = \frac{e^Z}{e^Z - 1} \quad (15)$$

where  $2d$  = gap width  
 = (0.89 mm)  
 = (35 mils)  
 $P$  = gap perimeter =  $2\pi r$   
 $L$  = specimen thickness  
 $Z = 2\pi d/L$   
 $r$  = meter area radius  
 = 0.2033 m  
 = 8.002 in

For  $L = 25$  mm (1 in),  $c = 0.021$  m (2.93 in). For  $L = 150$  mm (6 in),  $c = 0.030$  m (4.39 in). The measured value of

$$\begin{aligned} q_0 &\approx \frac{0.00057}{\mu\text{V}} \times \frac{1116}{\text{K}} \mu\text{V} \\ &\approx 0.64 \text{ W/K} \end{aligned} \quad (16)$$

For  $\lambda = 0.045$  W/m $\cdot$ K,  $c\lambda = 0.0013$  W/ $^\circ$ K at  $L = 152$  mm (6 in) and  $c\lambda = 0.0009$  at  $L = 25$  mm (1 in).

Thus  $c\lambda$  is expected to be smaller than  $q_0$ . Also the change in  $c\lambda$ , due to changes in  $L$  or  $\lambda$  is much smaller than  $q_0$ .

Looking again at the equation for the gap unbalance,

$$\frac{Q_g}{T_g} = S_g S_{tc} = q_0 + c\lambda \quad (17)$$

Thus,  $S_g \approx q_0/S_{tc}$ . Since  $q_0$  and  $S_{tc}$  are constants, independent of the sample,  $S_g$  is expected to be approximately constant for different sample material and thickness. This conclusion is confirmed by experimental results. The gap sensitivity,  $S_g$ , did not change by more than 5 percent between sample thicknesses of 25 mm (1 in) to 150 mm (6 in).

Another way to look at this result is that most of the heat flow across the gap ( $q_0$ ) flows directly across the gap, rather than through the sample ( $c\lambda$ ). The measured gap sensitivity is slightly larger than what would be expected, assuming that the heat flows entirely via the conduction mode only through the air in the gap. This is, of course, what would be expected, since there are support pins and temperature sensors in the gap.

Thus the order of magnitude values predicted by Woodside's [1] equations are roughly confirmed by experiment. It is important to note that the aforementioned method to determine the uncertainty of gap heat flow is strictly empirical. It is recommended that, for uncertainty analysis, this empirical method be generally used in place of a theoretical procedure.

### 3.5.5 $Q_{edge}$

Looking at the heat flow from the hot-plate, meter area, the difference between the ideal case with one-dimensional heat flow and the real case is due to the edge heat flow,  $Q_{edge}$ . Referring to figure 1, the ambient temperature,  $T_{amb}$ , is different from that of either the hot or cold plate. Usually,  $T_{amb}$  is equal to the average of the hot and cold plate temperatures,  $T_{mean}$ . At first glance, one would expect the net  $Q_{edge}$  to be zero when  $T_{amb}$  is equal to  $T_{mean}$ . This would be true if the heat flow were measured midway between the hot and cold plates. In fact, the heat flow is monitored at the surface of the hot plate. Some of the heat from the hot surface is going to the ambient, so the measured heat flow is greater than what would be the case for one-dimensional heat flow. Therefore, the ambient must be at a temperature higher than  $T_{mean}$ , for  $Q_{edge}$  to be zero.

This leads to the essential difficulty in estimating the edge effect, which is the issue of determining the value of  $T_{amb}$  at which  $Q_{edge}$  is zero. Figure 10 shows the plot of a theoretically calculated plot [3] of the percentage change in  $\lambda$  as the ambient temperature varies. Since  $\lambda$  is proportional to  $Q$ , the edge effect can be characterized by  $\lambda$  as well as  $Q$ . A value of zero for the ordinate corresponds to the case where  $\lambda$ -edge (or  $Q_{edge}$ ) equals zero. Note that this occurs when  $T_{amb}$  is greater than  $T_{mean}$ . It is possible to calculate the value of  $T_{amb}$  at which  $Q_{edge}$  is zero, and one such calculation is given in reference [3]. The next step is to consider how to check these calculations with experiment.

It is a simple matter to measure the slope of the curve in figure 10. It is more difficult to determine the zero crossing of the ordinate--at which (1)  $Q_{edge}$  equals zero or, equivalently, at which (2) the  $Q$  monitored at the hot

plate is equal to what it would be if the heat flow were one-dimensional or, equivalently, at which (3) one is measuring the "true" apparent thermal conductivity of the material,  $\lambda_0$ . The only way to determine this zero intercept is to put in a sample with a previously known  $\lambda$ -value. Two 150 mm (6-inch) specimens were measured on the NBS GHP. The edge effect is expected to be negligibly small at this 150 mm (6-inch) thickness, based on theory and experimental measurements of the slope of the curve in figure 10 (The value of this slope was less than 0.06 percent/ $^{\circ}$ K). Therefore, the  $\lambda$ -value of each 150-mm (6-inch) sample is known within the experimental uncertainty at this thickness.

The next step in the experiment was to stack the two 150 mm (6-inch) specimens to make a 12-inch sample. The mean temperature was 23.9 C (75 F), and the plate temperature difference ( $T_{\text{hot}} - T_{\text{cold}}$ ) was 27.8 C (50 F). At this thickness, for the NBS GHP, the edge effect was expected to be significant ( $\sim 0.4$  percent change in  $\lambda$ -value for a  $1^{\circ}$ C change). A zero value of the abscissa in figure 10 corresponds to the ambient temperature being equal to the mean temperature. A theoretical calculation [3] indicated that the corresponding value of the ordinate [3] would be  $\sim 0.07$  percent. Preliminary experimental values were  $\pm 0.5$  percent, about the expected value. The slope of the experimental curve was about 25 percent greater than that of the calculated curve.

It should be possible to use an experimental curve similar to that in figure 10 to estimate the value of the abscissa (which is proportional to  $[T_{\text{mean}} - T_{\text{ambient}}]$ ) at which the measured  $\lambda$  is equal to  $\lambda_0$ . According to theory, the ambient temperature should be less than the mean temperature to measure the true  $\lambda$ -value ( $\lambda - \lambda_0 = 0$ ). The uncertainty, as far as the edge effect is concerned, with which  $\lambda_0$  is known might be estimated as follows. The uncertainty in the measured value of  $\lambda_0$  is estimated simply as the sum of the uncertainty of the measured value of the abscissa and that of the ordinate. The uncertainty of the ordinate is based on the uncertainties of the two measured  $\lambda$ -values at 150 mm (6 inches). The part of these uncertainties that is systematic will cancel since the ordinate is a ratio. The remaining part is the repeatability of the measured  $\lambda$ -value at 150 mm (6 inches), when the sample is removed from and replaced in the apparatus. This repeatability was measured to be within 0.2 percent. The uncertainty in the abscissa is essentially equal to that of the measured ambient temperature, since the mean temperature is known much more accurately. The ambient temperature was measured with a differential thermocouple in conjunction with a good absolute sensor. Since the ambient temperature was not constant around the plates, the thermocouple stages were uniformly distributed to measure the average ambient temperature. A comparison of an average based on 4 points agreed within 0.3 K (0.6 F) with an average based on 24 points. The uncertainty in the ambient temperature was estimated at 0.3 K (0.6 F). Using the value of the slope in figure 10, this corresponds to about a 0.2 percent uncertainty in the ordinate. The sum of the two parts was 0.4 percent. A slightly larger value of 0.5 percent was used in table 2 as the estimate of the upper-bound uncertainty of a measured  $\lambda$ -value at 300 mm (12 inches), due to edge effects. Further experimental work must be performed in this area.

### 3.6 TEMPERATURE MEASUREMENT

#### 3.6.1 Overview

In order to calculate the apparent thermal conductivity,  $\lambda$ , via equation (2), one must measure the plate temperatures. Platinum resistance thermometers (PRT's) and thermocouples are used in this measurement. The PRT is used to determine the absolute temperature at a particular plate location, and differential thermocouples are used to measure the relative temperatures between the PRT and other locations. The discussion of the uncertainties of the average, meter-area, plate-temperature values follows the discussion of the uncertainties of the PRT and thermocouples values.

#### 3.6.2 PRT Circuit Rationale

Platinum resistance thermometers are used to measure the absolute temperature in the meter area of the hot and cold plates. These PRT's were 3 mm in diameter and 6 mm in length. The circuit in figure 11 is used to measure the PRT resistance values. The standard resistor,  $R_{std}$ , is manufactured by the Leeds and Northrup Company of North Wales, Pennsylvania, Catalog #4030-B, Serial #1875050. It was calibrated in March, 1980 to have a value of  $99.9992 \Omega$  at the average oil bath temperature of 24 C. Assuming that the oil bath, which surrounds  $R_{std}$ , is maintained within  $\pm 2$  K, the resistance is constant within  $\pm 15$  ppm or  $\pm 0.001$  percent.

The value of the PRT resistance,  $R_x$ , is  $R_x = (V_x/V_{std}) R_{std}$ . Note that the DVM voltage uncertainty due to the zero uncertainty is effectively eliminated by taking the ratio. Also the DVM uncertainty due to linearity is effectively eliminated by matching the values of  $R_x$  and  $R_{std}$ . Thus, the readout percentage uncertainty of  $R_x$ ,  $\Delta R_x$ , is approximately equal to that of  $R_{std}$ , which is  $\pm 0.001$  percent. Since a change of  $1 \Omega$  corresponds to a change of about 2 K for these "100  $\Omega$ " PRT's, the value of 0.001 percent corresponds to 1 milli-ohm or 2 milli-Kelvin (mK).

#### 3.6.3 PRT Calibration

The PRT's were calibrated by the National Bureau of Standards at six temperatures between 0°C and 50°C. The calibration points were fitted to the equation

$$T = a + bR + cR^2 \quad (18)$$

where  $T$  is the temperature corresponding to the IPTS-68 temperature and  $R$  is the PRT electrical resistance. The equation coefficients were evaluated by a least-squares fit. The residual standard deviation multiplied by 3 corresponded to a range of 3 to 5 mK, which agreed with the quoted calibration uncertainty of 5 mK. Any systematic error in the NBS bath calibration set-up would be expected to fall within the above range. The calibration uncertainty is then estimated at  $\Delta_{cal} = 5$  mK. Any calculational uncertainty using equation (18) is expected to be negligible.

The model number of the PRT's is S-1059-2. They were produced by the MINCO Corporation. There is a quoted uncertainty value of 1 mK for 20 temperature cycles between plus and minus 200°C. This must, of course, be checked by a calibration history. The agreement between calibration values of September 1980 and December 1981 was within 3 mK, which was within the above-mentioned calibration uncertainty. Since the PRT's are cycled only between -14°C and +51°C and since the calibration history does not indicate any detectable change, the contribution to uncertainty due to re-cycling will be considered negligible.

#### 3.6.4 PRT Self-Heating Uncertainty

The PRT's have a current of 1 mA, which heats the medium around them (external self-heating) and the sensor itself (internal self-heating). The external self-heating is negligible. That is, the conductivity and the heat capacity of the aluminum plate surrounding the PRT is large enough to carry away the PRT-generated heat without raising the nearby plate temperature a measurable amount. The order of magnitude of the internal self-heating can be estimated by the "rule of thumb" formula-- $\Delta T(\text{in mK}) = 0.4/I(\text{in mA})$ . Thus, for the PRT,  $\Delta T$  would be about 0.5 mK. However, the self-heating in the calibration would be expected to be about the same as in the measurement, since the current is 1 mA in each case. Thus, the external self-heating is already taken into account in the temperature determination, and its contribution to the temperature uncertainty is considered to be negligible.

#### 3.6.5 Temperature Distribution Over Meter Area

The temperatures are measured at a point near the center of the meter area of the hot plate and the two cold plates. This measurement is accomplished with the PRT's described in the previous section. This next section considers the question of the difference between this temperature at the center point and the average temperature over the whole meter area.

The theoretical temperature distribution,  $T(r, \theta)$ , for the hot-plate meter area is given in reference [3]. The design and construction of the hot and cold plates are also discussed. The salient features are that the cold plate has imbedded within it milled channels of a double spiral shape. Ethylene-glycol fluid is circulated through these channels to maintain the plates at a particular temperature. The double spiral shape of the tubing was chosen to have a more constant (than a single spiral) temperature ( $T$ ) over the meter area. A thermopile was used to check the temperature differences between various points on the surface of the cold plate. This difference was measured to be less than 10 mK, and this is the  $T$ -distribution uncertainty for the cold plates.

The hot plate is heated by a ribbon-shaped heater located at a distance from the center of about 0.71 times the gap radius. This heater goes around the center in a circular shape. Thus, the hot plate is relatively hotter at the heater position than at either the center or gap position (see figure 12). The location of the heater was chosen so that the gap temperature would be equal to the average temperature over the whole meter area [3]. The circular geometry was chosen to have azimuthal symmetry for the temperature distribution in the

meter area. This will not be exactly true due to heat sources or leaks which do not preserve this symmetry--such as the incoming heater leads or the support pins in the gaps. Thus, there is expected to be some angular distribution (~5 mK for a worst case of a 1-inch insulation sample).

In order to check the calculations of the temperature distribution it is desirable to have a measurement precision better than the expected T differences (~5-30 mK). Chromel-Constantan thermopiles with 16 stages were chosen. These had a sensitivity of about 1 mK/ $\mu$ V. Since the voltage measurement accuracy is ~ 1 $\mu$ V, there should have been about a 1 mK read-out resolution. There were two such thermopiles--one with a 2-inch span and another with a 6-inch span. These were constructed so that the thermocouple beads would rest on the hot-plate surface. It is important to use rigid samples to press the thermopile against the plate surface. Also, since there is a significant temperature gradient perpendicular to the plates (i.e., in the z direction), there are two components to the thermopile voltage. One is due to the plate temperature, and the other to the bead position. The former changes with the thermopile orientation on the plate, and the latter does not. This is probably due partly to a difference in the average z-position of the beads on the two sides of the thermopile and partly to a difference in the contact, and hence, contact thermal resistance between the thermopile junctions and the plates. To eliminate this constant bias (it varied between 10-80 $\mu$ V), thermopile readings were taken in the normal orientation and then with the thermopile rotated 180°. This technique gave a repeatability of  $\pm$  10 mK. Based on this data the estimate of the upper bound for the difference between the temperature at these locations and that over the cold-plate, meter-area is 15 mK. The PRT's in the cold plate are located 2 inches from the center of the plates.

Next, a check was made to ascertain that the temperature of the hot plate at the gap is equal to the average over the meter area. Referring to figure 13, the calculation in reference [3] indicated that the ratio of the temperature difference between the center and the heater location,  $\Delta y$ , and the temperature difference between the gap and the heater location,  $\Delta x$ , should be 1.6. The measured value of this ratio was  $1.6 \pm 0.3$ . Thus, the temperature at the gap is at the point, between the highest and lowest points, where it should be according to theory. A value of  $\pm$  15 mK is ascribed to the uncertainty due to the average meter-area temperature being approximated by the temperature of the PRT at the gap. This is essentially the uncertainty of the thermopile measurement technique described in the previous paragraph. The model may very well predict the average temperature much better, but it is difficult to confirm by experiment.

The order of magnitude of the maximum temperature difference in the hot plate,  $\Delta y$  (between the center and heater positions), was calculated to be ~250 mK for a value of heat flow per unit area,  $Q/A$ , of 90 W/m<sup>2</sup> [3]. This  $Q/A$  corresponds to a low-density, 25 mm (1 inch) insulation specimen measured in the two-sided configuration. The measured value in this case was ~60 mK. Thus, the temperature in the meter area was about 4 times more uniform than expected. It may be that the models do not give a good prediction for temperature differences less than ~100 mK.

An additional point relates to the high gradient in the gap, which was discussed in the section on the gap. It is important to locate the PRT used for the hot plate, meter-area temperature measurement on the meter-side of the gap, before the temperature gradient makes the sharp increase. Remember that the temperature differences measured above are for the worst case of  $Q/R = 90 \text{ W/m}^2$ . These differences decrease inversely with  $Q/A$ . The worst case value is used as an upper-bound estimate of the uncertainty in the following summary.

Another possible source of error is due to the fact that the hot plate PRT is located in the center of the gap, midway between the plate surfaces upon which the samples rest. Refer to figure 14. If there is any thermal gradient in the z-direction, then the temperature at the PRT location would be slightly different from the average surface temperature over the meter-area surface. In reference [3] a calculation is performed that indicates that this difference is negligible ( $< .01$  percent) for the sample conductivities typically measured ( $< 0.4 \text{ W/m}\cdot\text{K}$ ).

### 3.6.6 Summary of Temperature Uncertainties

Let us sum the various contributions,  $\Delta T$ , to the uncertainty in the measurement of the average  $T$  over the meter-area.

$\Delta T$ due to PRT resistance	<u>2</u> mK
$\Delta T$ due to bath calibration	<u>5</u> mK
$\Delta T$ due to temperature distribution not constant	
hot plate	<u>15</u> mK
(cold plate)	<u>15</u> mK
TOTAL-hot plate	<u>22</u> mK
-(cold plate)	<u>22</u> mK

### 3.7 PLATE EMITTANCE

The amount of heat flow that goes across the sample depends on the emittance of the hot and cold plates. For the NBS GHP plates a value of normal plate emittance at room temperature in the visible was measured to be  $0.89 \pm .02$ . Admittedly, this could be different from the value of the hemispherical emittance in the infrared ( $3\mu\text{-}30\mu$ ) which is appropriate to the following equation. This equation calculates the apparent thermal conductivity,  $\lambda$ , as a function of density,  $D$ , thickness,  $L$ , and plate hemispherical emittance,  $\epsilon$ , and it is derived in reference [4].

$$\lambda = a + bD + \frac{4\sigma\bar{T}^3}{3/4 \beta + \frac{1}{L \epsilon} (2 - 1)} \quad (19)$$

Here,  $\beta$  is the extinction coefficient, "a" is approximately equal to the thermal conductivity of air, "b" is due to conduction thru the solid fibers,  $\bar{T}$  is the mean temperature in the sample and  $\sigma$  is the Stefan-Boltzmann constant. In SI units,

$$a \approx .026 \text{ W/m}\cdot\text{K}$$

$$\bar{T} = 297.0 \text{ K}$$

$$b = 0.009 \text{ W}\cdot\text{m}^2/\text{K}\cdot\text{kg}$$

$$\beta = 328 \text{ m}^{-1}$$

In English units,

$$a = .18 \text{ Btu}\cdot\text{in}/\text{hr}\cdot\text{ft}^2\cdot^\circ\text{F}$$

$$T = 75^\circ\text{F}$$

$$b = 0.004 \text{ Btu}\cdot\text{in}\cdot\text{ft}/\text{lb}\cdot\text{hr}\cdot^\circ\text{F}$$

$$\beta = 100 \text{ ft}^{-1}$$

The fitted values of "a" and "b" will vary with product. The purpose here is to evaluate the change in  $\lambda$ -value for a change in  $\epsilon$ . Hence, it is sufficient that the values have the correct order of magnitude. For a sample with  $D \approx 9 \text{ kg/m}^3$  ( $0.6 \text{ lb/ft}^3$ ), if  $L \approx 25 \text{ mm}$  (1 inch) the percentage change in  $\lambda$ , when  $\epsilon$  changes from 0.89 to 0.87, is 0.25 percent. For  $L \approx 150 \text{ mm}$  (6 inch), the same change is 0.05 percent. For a sample with  $D \approx 130 \text{ kg/m}^3$  ( $8 \text{ lb/ft}^3$ ), the percentage change in  $\lambda$  is 0.003 percent at  $L = 1 \text{ in}$ . The point of this exercise is to show that an uncertainty in  $\lambda$ -value due to an uncertainty in  $\epsilon$  is significant for low-density material at  $L = 25 \text{ mm}$  (1 inch). It is not significant for  $L = 150 \text{ mm}$  (6 in), and it is not at all significant for high density material.

This point is sufficiently important and subtle to warrant a more detailed discussion. In the case where there is a significant radiation heat transfer through a sample, the measured R-value and apparent  $\lambda$ -value depend on the emittance of the plates. For a higher value of  $\epsilon$ , there is more heat conducted thru the sample. Thus, the measured R-value is dependent on an apparatus parameter.

This has a bearing on the matter of comparison among different apparatuses. Ideally, one measures a quantity that does not depend on the apparatus. Then, a similar measurement on an identical sample should give an identical result.

Using the previously described model, for the case of a low-density, 1-inch sample, a difference in  $\epsilon$  from 0.9 to 0.8 results in a percentage difference in  $\lambda$ -value of 1.2 percent. Clearly, one could have significant errors in a round-robin, apparatus comparison, if the values of  $\epsilon$  were not considered.

One way to circumvent this problem is to standardize the values of  $\epsilon$  for the apparatuses. This is encouraged in the ASTM test methods for the guarded-hot-plate and heat-flow-meter apparatus, which require that the value of  $\epsilon$  be equal to 0.9. The estimate of  $\epsilon$  must be based on an actual measurement. Care must be taken to specify whether the normal or the hemispherical emittance is

measured, as these might differ by about 10 percent. It is recommended that the hemispherical emittance ( $3-30\mu$ ) be measured, since it is the quantity appropriate to equation (19).

Even if the  $\epsilon$ -values of two apparatuses have been measured to be the same, there is an uncertainty in their  $\lambda$ -value comparison due to the uncertainty in the measured  $\epsilon$ . In the case where the  $\epsilon$ -values for two apparatuses are different, one can use a model like the one presented earlier to estimate the corresponding adjustments in  $\lambda$ -value. A final solution is to use samples of greater thickness or density, where the uncertainty of  $\lambda$  due to that of  $\epsilon$  is negligible.

#### 4. TOTAL UNCERTAINTY

In this section, the various uncertainties will be combined to give an overall uncertainty. Table 1 contains the individual and total uncertainties for a range of test conditions, and this section will explain these values. Each individual uncertainty is treated as an upper bound on the random plus systematic uncertainties. A value of  $3s$  is used for the random part, where  $s$  is estimate of the standard deviation. The upper bound estimates are simply added to estimate the upper bound of the total uncertainty. The individual percent uncertainties in  $\lambda$  are the ratio of the uncertainty over the variable, e.g.,  $\Delta A/A$ .

The uncertainty in the area determination,  $\Delta A$ , is  $1.3 \times 10^{-5} \text{ m}^2$ , which corresponds to a 0.01 percent uncertainty in  $\lambda$ .

For compressible samples the thickness uncertainty,  $\Delta L$ , is  $25 \text{ }\mu\text{m}$  (1.0 mil). Thus the percent uncertainty is 0.1 percent for  $L = 25 \text{ mm}$  (1 in) and  $\sim 0.01$  percent for  $L = 300 \text{ mm}$  (12 in).

The uncertainty in the power generated by the hot-plate, meter-area heater,  $\Delta Q_m$ , is 0.04 percent. Remember, it is primarily due to the measurement of the voltage across the  $0.1 \text{ }\Omega$  shunt resistor, on the 100 mV range of the digital voltmeter, and it does not change significantly over the range of power values.

The uncertainty due to the heat generated by resistive devices,  $\Delta Q_r$ , in the hot plate meter area is 0.4 mW. This corresponds to 0.04 percent to 0.004 percent for power values of 1 W to 10 W.

The uncertainty in the heat flow across the gap,  $\Delta Q_g$ , is 0.3 mW. This corresponds to  $0.5 \text{ }\mu\text{V}$  for the gap voltage uncertainty. The percent uncertainty varies from 0.03 to 0.003 as the gap power varies from 1 W to 12 W. The uncertainty due to the edge heat flow,  $\Delta Q_{\text{edge}}$ , is negligible up to thicknesses 150 mm (6 in). At a thickness of 300 mm (12 in),  $\Delta Q_{\text{edge}}$  is estimated to correspond to 0.5 percent.

The uncertainty of both the hot and cold plate temperature is 22 mK. The difference between hot and cold plate temperatures is used to calculate the thermal resistance, so the value of 22 mK for the hot plate is added to the 22 mK for the cold plate to arrive at a value of 44 mK for the temperature difference uncertainty,  $\Delta(T_h - T_c)$ . A typical value for  $(T_h - T_c)$  is 27.8 K (50 F), in which case the percent uncertainty is 0.16 percent.

For the purpose of comparison among different apparatuses, the uncertainty in measured plate emittance of 2 percent corresponds to an uncertainty in thermal resistance,  $\Delta R$ , of 0.25 percent at  $L = 25 \text{ mm}$  (1 in), 0.05 percent at  $L = 150 \text{ mm}$  (6 in) and 0.02 percent at  $L = 300 \text{ mm}$  (12 in). (Remember that the uncertainty would be negligible for high-density material.)

The values given in table 1 are for low-density samples with an apparent thermal conductivity of  $0.046 \text{ W/m}\cdot\text{K}$  ( $0.32 \text{ Btu-in/hr}\cdot\text{ft}^2\cdot\text{F}$ ) at thicknesses of 25, 75, 150 and 300 mm (1, 3, 6 and 12 in) which correspond to meter power ( $Q_m$ ) values

of 12, 4, 2 and 1 W, for two-sided operation. For one-sided operation,  $Q_m$  is 6, 2, 1 and 0.5 W, respectively.

The values of total uncertainty are 0.31 percent for  $L = 25$  mm (1 inch), 0.26 percent for  $L = 75$  mm (3 inches), 0.27 percent for  $L = 150$  mm (6 inches) and 0.79 percent for  $L = 300$  mm (12 inches).

## 5. VERIFICATION OF UNCERTAINTY ESTIMATE

It is appropriate here to discuss the philosophical aspects of the accuracy issue. The assumption is made that a sample has a particular "true" value for its thermal resistance, or equivalently for its apparent thermal conductivity. The question is, "How closely does a data point measured on an apparatus approximate the "true" value?"

Before addressing this question, let us define two basic kinds of uncertainty--random and systematic. Suppose a large number of  $\lambda$ -value data points are measured, and that these points are distributed about an average value in some Gaussian-like distribution. The uncertainty of the knowledge of the average value is characterized by a standard deviation. Even if the average of this distribution were known exactly, it would still not necessarily be equal to the "true" value. This is due to systematic errors in the measured values. Systematic errors are not known, and one can not reduce them by repeating many tests. The only way to learn about them is to make an independent measurement on an identical sample with another apparatus of better or comparable accuracy. If there is agreement among a number of apparatuses within the calculated uncertainties, then the uncertainty estimates, and the corresponding model, can be considered to be verified, in so much as is possible.

We at NBS look forward to participating in comparisons between our apparatus and other apparatuses, and this will certainly be done in a definitive manner in the near future. A major difficulty is to ensure that the samples are identical. Important sample requirements are durability and uniformity. The moisture content should also be the same.

It is, on the other hand, possible to determine the random uncertainty with many measurements on a single apparatus. Repeated measurements on the same sample give an indication of the overall random uncertainty. These can be done for a short-term (e.g., 1 week) or a long term (e.g., several years). The long-term variation might reveal a long-term drift in a systematic error. The short-term repeatability was measured with 100 mm (4 in) samples of low-density insulation to be 0.1 percent. Again, this repeatability serves as an estimate of the random part (or the precision) of the overall uncertainty. The estimates of uncertainty in the previous sections have been upper bounds on the possible errors. For the most part they have been systematic in nature although they include random parts.

Generally speaking, the data on a single test has two parts. The transient part at the beginning of the test shows a monotonically increasing or decreasing curve. When there is no monotonic trend, the steady state condition has been achieved. There is still a scatter of data points due mostly to the cycling of the bath temperatures. The scatter band is about 1 mK for the hot plate temperature, 6 mK for the cold plate temperatures and 1 mW for the power. The scatter in the calculated  $\lambda$ -value is about 0.01 percent for a two-sided, 1-inch sample and 0.03 percent for a two-sided, 6-inch sample. The mean value is, of course, known even better. Clearly, the scatter in the data points, after the steady state condition is attained, is negligible compared to the estimated systematic errors in the  $\lambda$ -value.

## 6. REFERENCES

1. Woodside, W., and Wilson, A. G., "Unbalance Errors in Guarded Hot Plate Measurements," Symposium on Thermal Conductivity Measurements and Applications of Thermal Insulations, ASTM STP 217, ASTTA, Am. Soc. Testing Mats., 1957, pp. 32-48.
2. Woodside, W., "Deviations from One-Dimensional Heat Flow in Guarded Hot Plate Measurements," Review of Scientific Instruments, RSINA, Vol. 28, 1957, pp. 1933-1937.
3. Hahn, M. H., Robinson, H. E., and Flynn, D. R., "Robinson Line-Heat-Source Guarded Hot Plate Apparatus," Heat Transmission Measurements in Thermal Insulations, ASTM STP 544, American Society Testing and Materials, 1974, pp. 167-192.
4. Brian G. Rennex, "Thermal Parameters as a Function of Thickness in Low-Density Insulation," Journal of Thermal Insulation, Vol. 3, pp. 37-62, 1979.

Table 1. Percentage Estimate of Uncertainties in the Measured Apparent Thermal Conductivity for the NBS Guarded Hot Plate

Quantitative Value	Thickness			
	25 mm (1 inch)	75 mm (3 inches)	150 mm (6 inches)	300 mm (12 inches)
	Percent Uncertainty			
Area (12 $\mu\text{m}$ or 0.5 mil in radius)	0.01	0.01	0.01	0.01
Thickness (25 $\mu\text{m}$ or 1.0 mil)	0.1	0.03	0.02	0.01
Meter Power	0.04	0.04	0.04	0.04
Meter Resistive Device (0.4 mW)	0.00	0.01	0.02	0.04
Gap Heat Flow (0.3 mW, or 0.5 $\mu\text{V}$ in gap voltage)	0.00	0.01	0.02	0.03
Edge Heat Flow	0.00	0.00	0.00	0.50
Hot, cold-plate Temperature Difference (44 mk)	0.16	0.16	0.16	0.16
TOTAL	0.31	0.26	0.27	0.79

\* These values are for compressible, low-density, glass-fiber insulation measured in the two-sided mode with a plate temperature difference of 28 K. Uncertainty values of less than 0.01 percent are reported as zero.

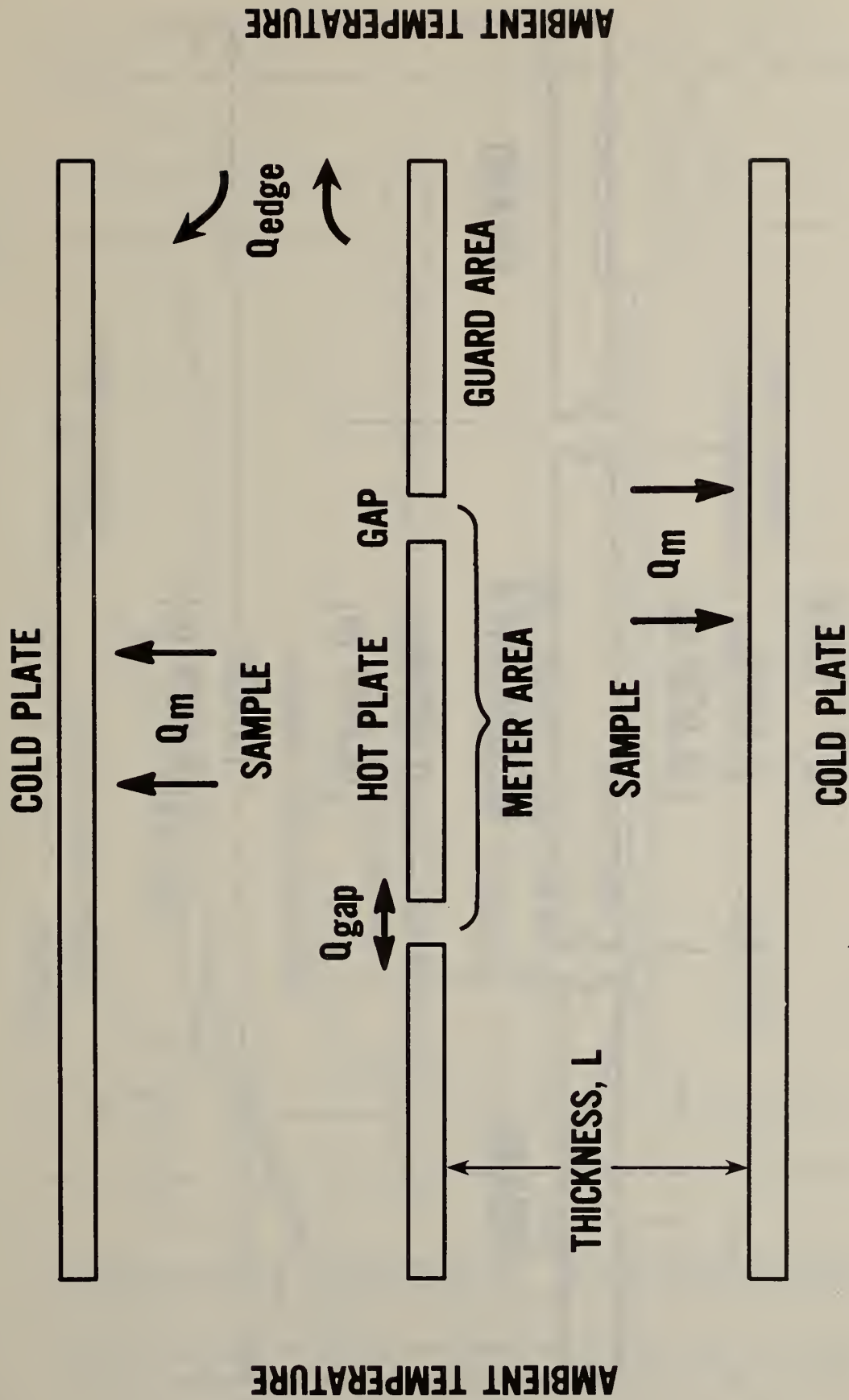
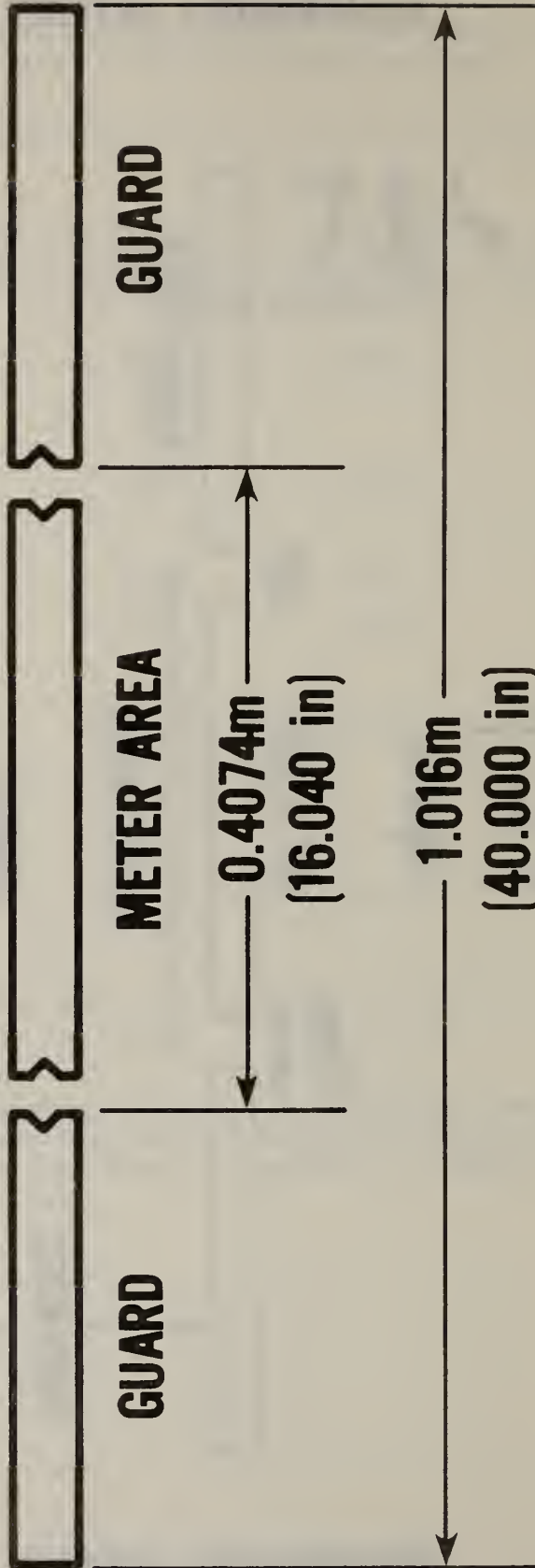


FIGURE 1 HEAT FLOW ( $Q$ ) IN A TWO-SIDED GUARDED HOT PLATE

**HOT PLATE**

0.4056m  
(15.970 in)



**GUARD**

**METER AREA**

0.4074m  
(16.040 in)

**GUARD**

1.016m  
(40.000 in)

FIGURE 2 SIDE VIEW OF GAP

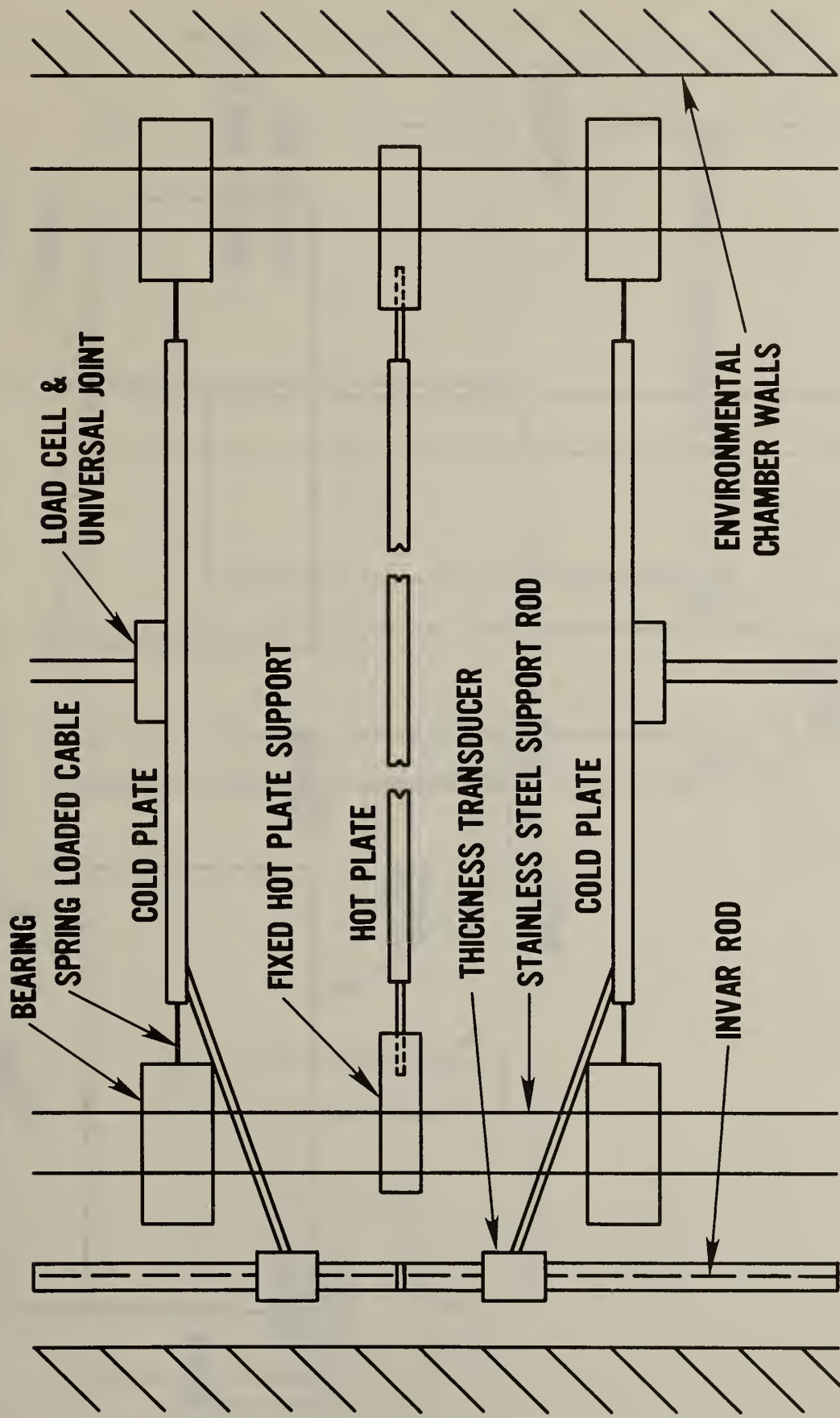


FIGURE 3 PLATE SUPPORT AND THICKNESS CALIBRATION

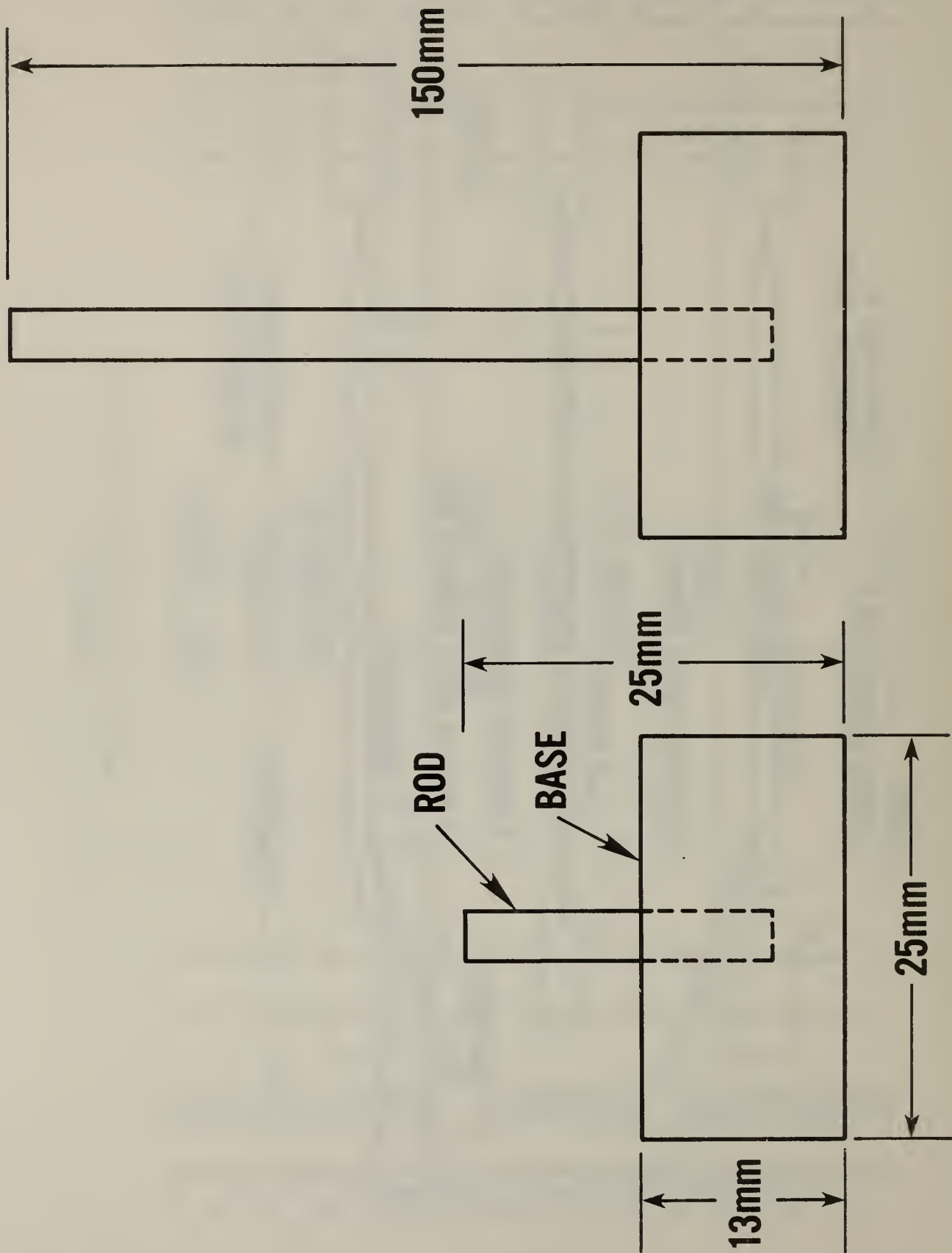


FIGURE 4 THICKNESS TRANSDUCER FOR L-MAP

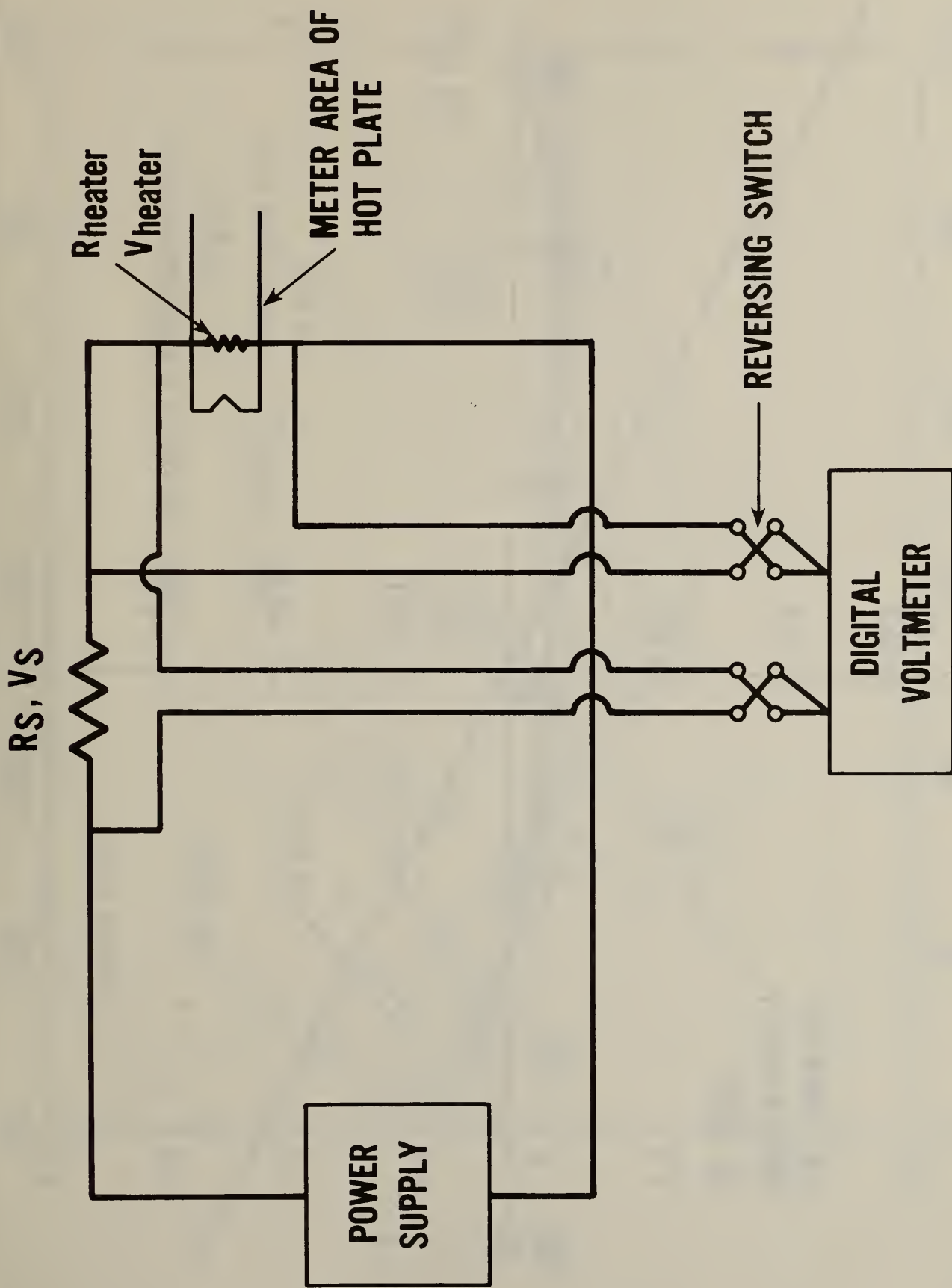


FIGURE 5 CIRCUIT FOR METER-AREA POWER MEASUREMENT

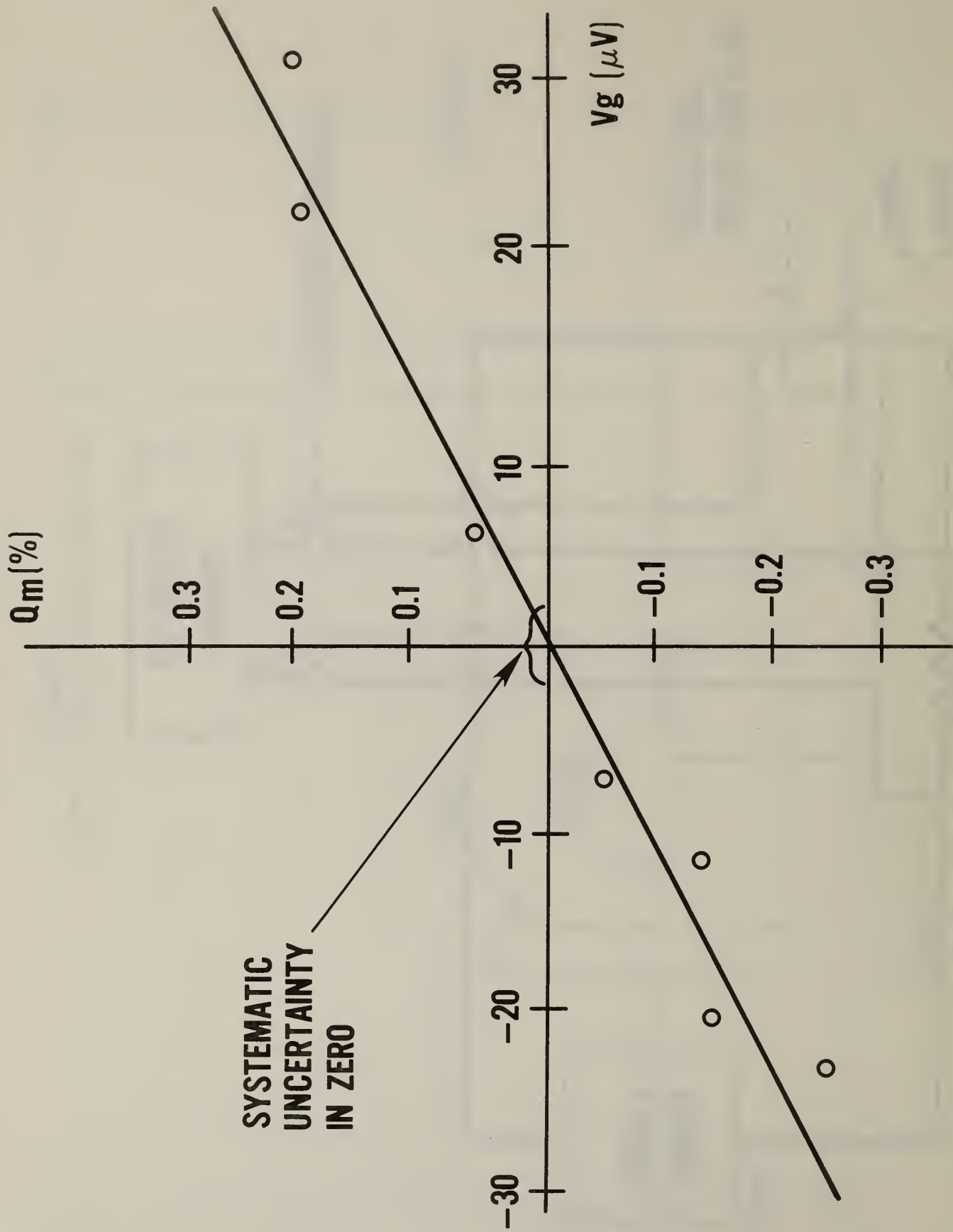


FIGURE 6 HOT-PLATE, METER-AREA POWER,  $Q_m$ ,  
VERSUS GAP VOLTAGE

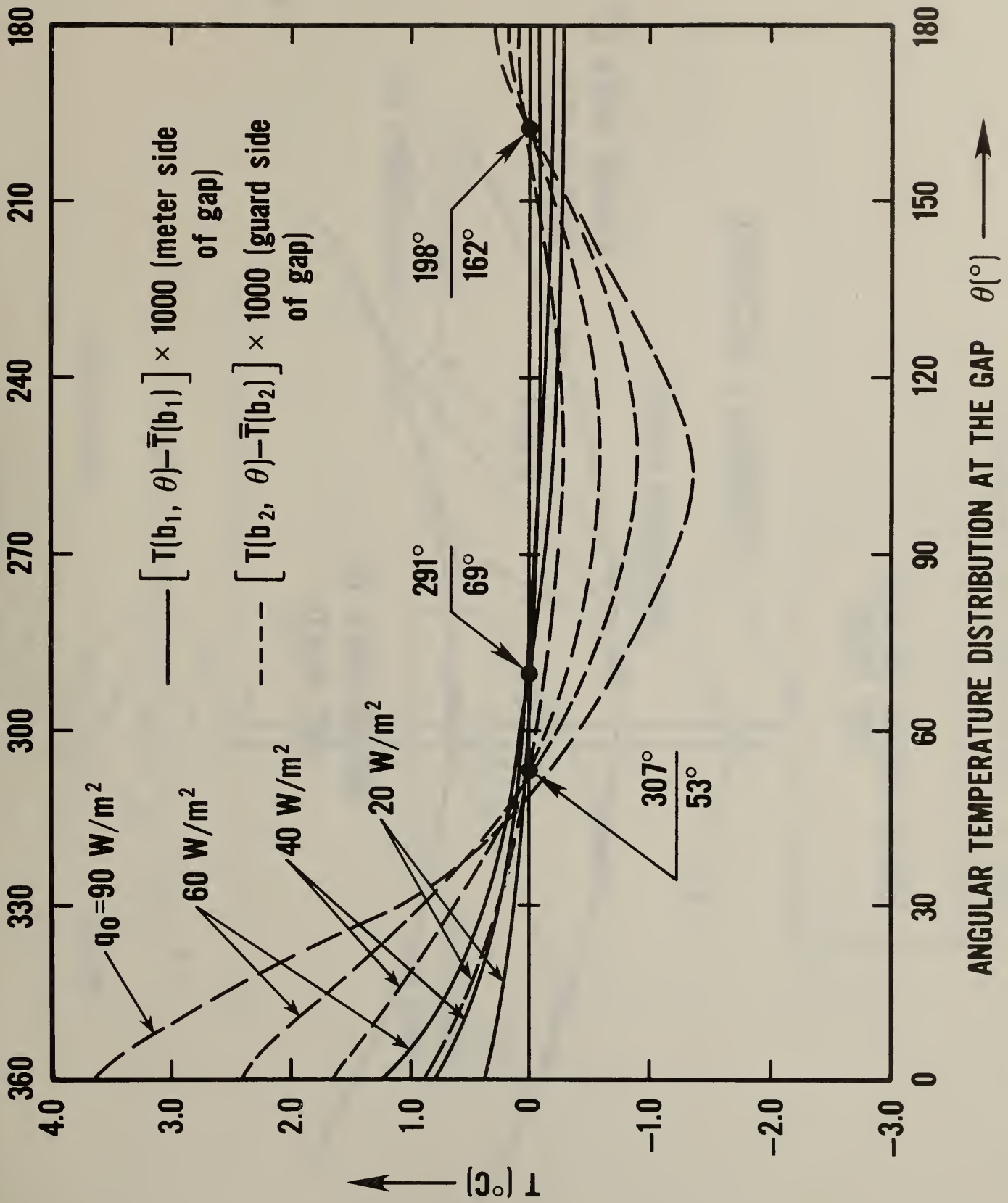


FIGURE 7 CALCULATED ANGULAR TEMPERATURE DISTRIBUTION AT GAP

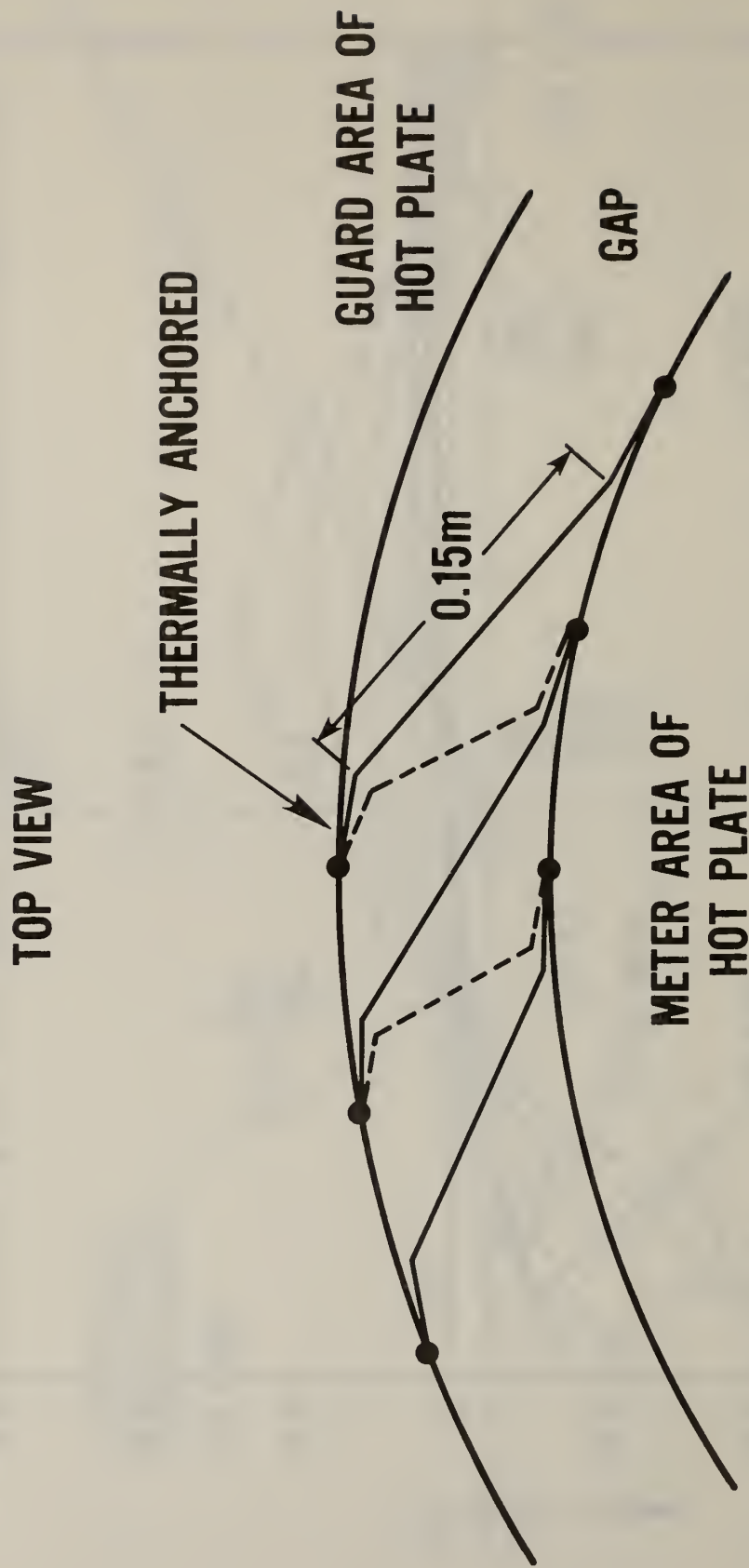


FIGURE 8 DIAGRAM OF GAP THERMOPILE JUNCTIONS

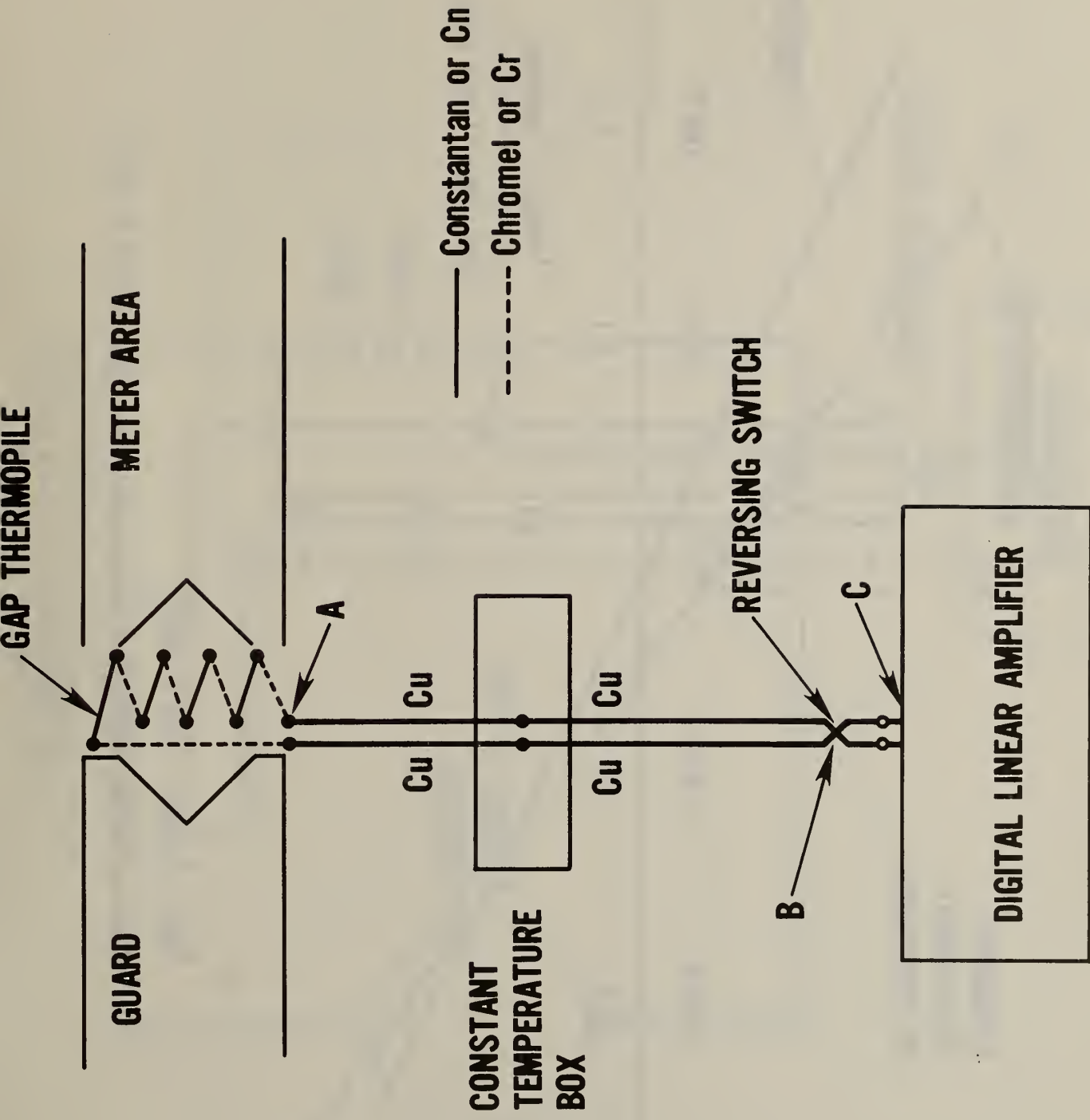
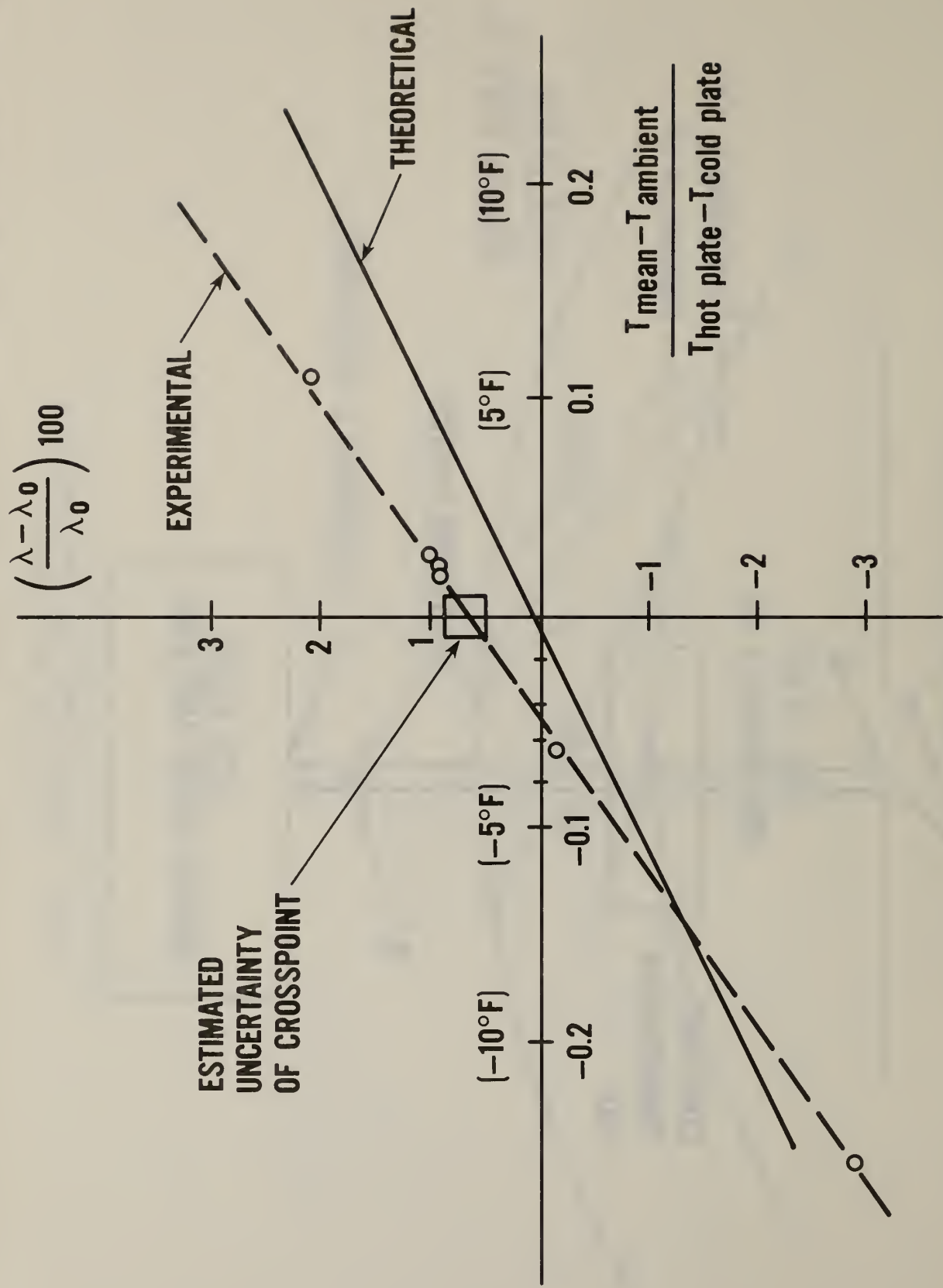


FIGURE 9 VOLTAGE CIRCUIT AND WIRE CONFIGURATION FOR THE GAP THERMOPILE



$T_{\text{hot}} - T_{\text{cold}} = 27.8^\circ\text{C} (50^\circ\text{F})$

The  $\lambda_0$  is the estimated value when the edge effect is zero

FIGURE 10 THE CHANGE IN APPARENT THERMAL CONDUCTIVITY,  $\lambda$ , AS A FUNCTION OF AMBIENT TEMPERATURE\*

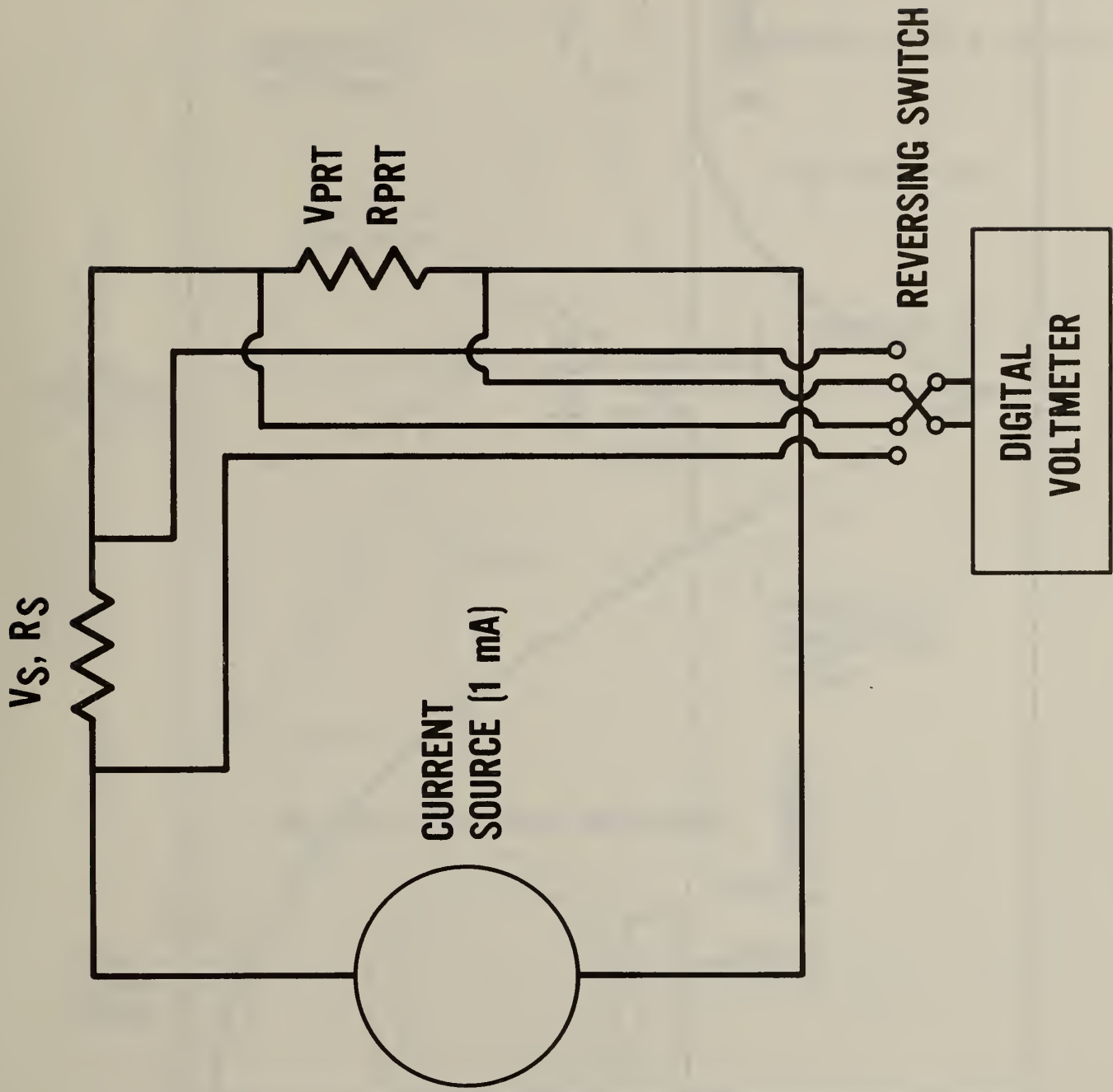


FIGURE 11 CIRCUIT FOR THE PLATINUM-RESISTANCE THERMOMETER (PRT) RESISTANCE MEASUREMENT

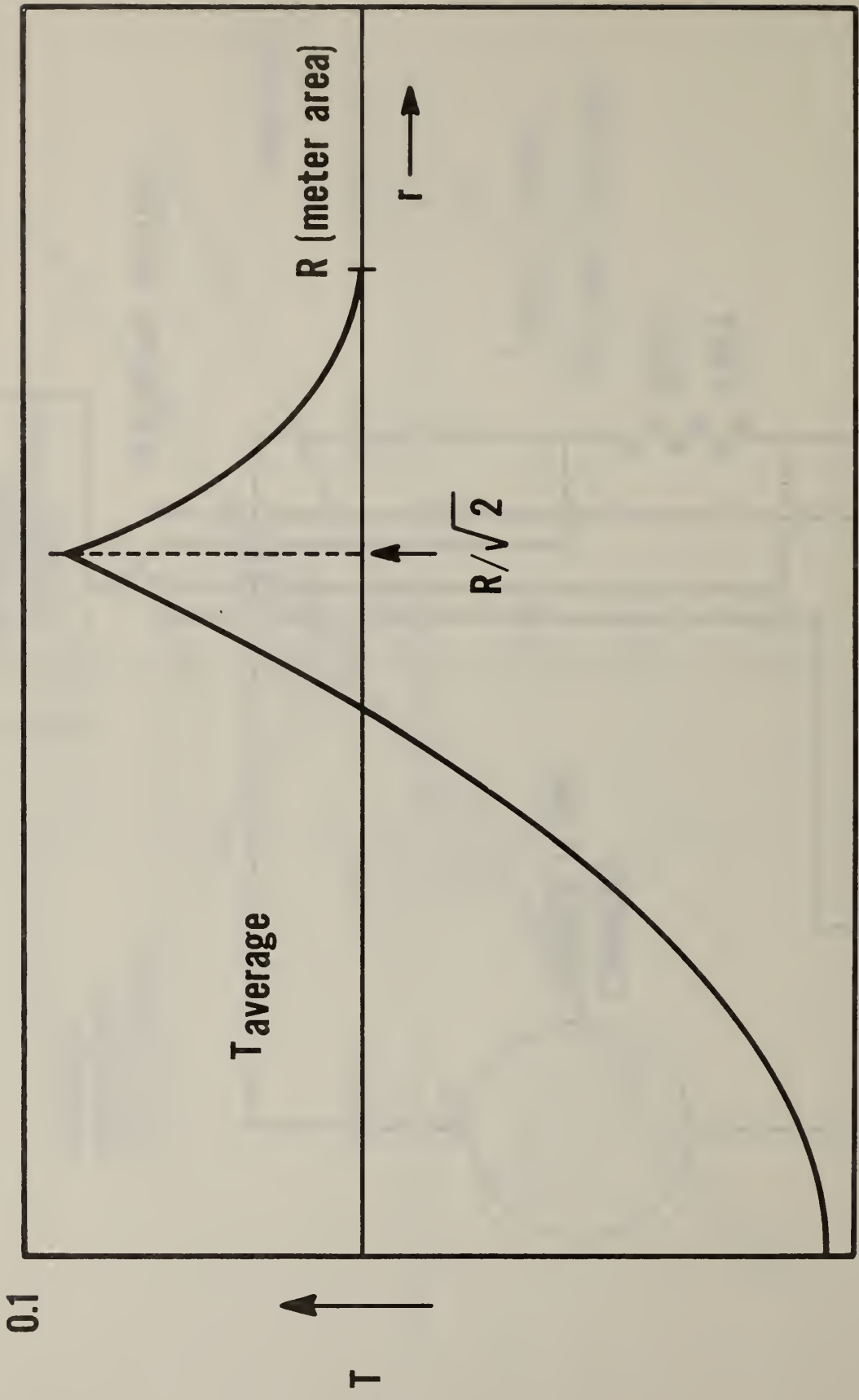
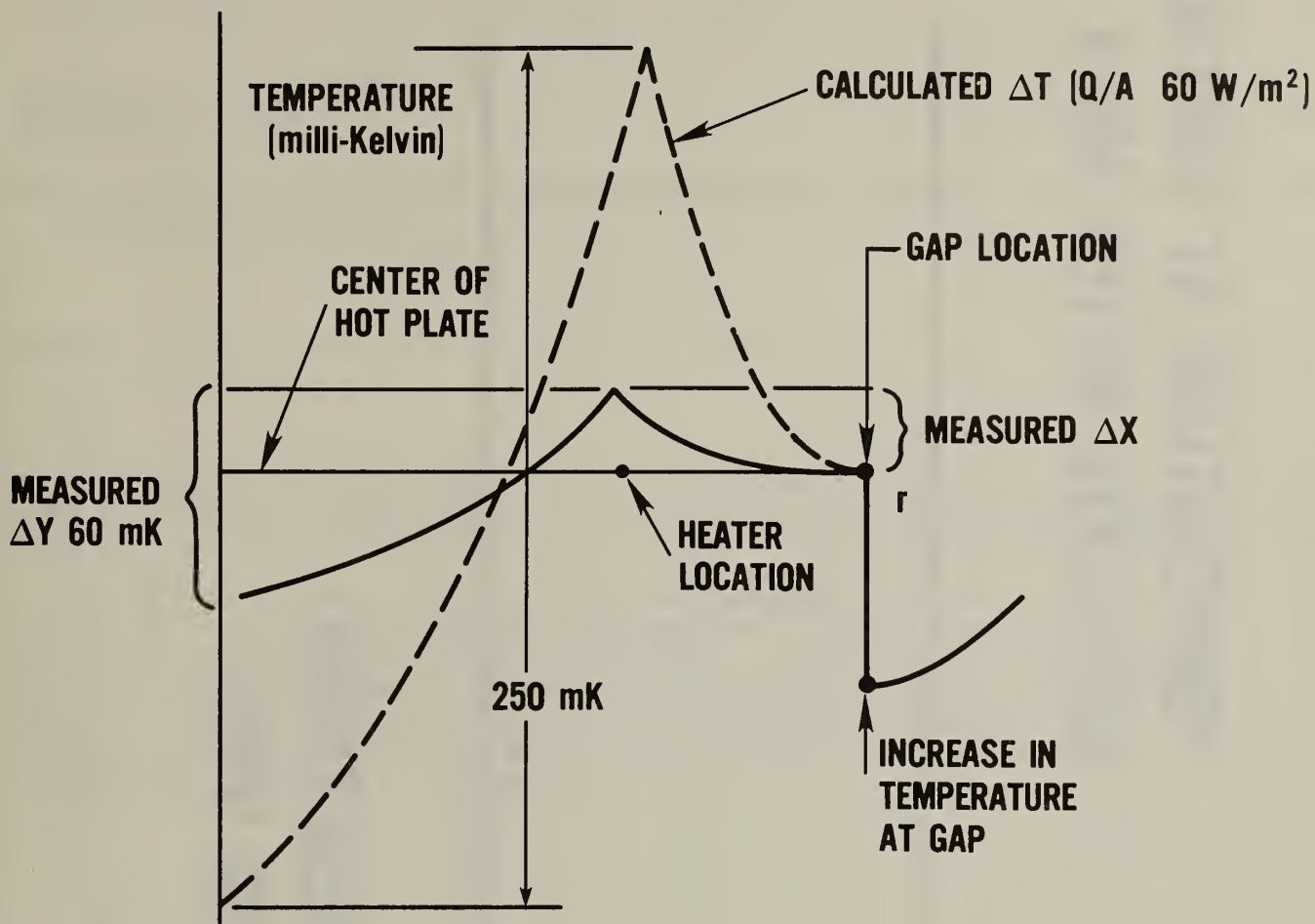


FIGURE 12 THEORETICAL PLOT OF THE HOT-PLATE, METER-AREA RADIAL TEMPERATURE DISTRIBUTION



TOP VIEW OF HOT PLATE METER AREA

$$\frac{r_{\text{gap}}}{r_{\text{heater}}} = \sqrt{2}$$

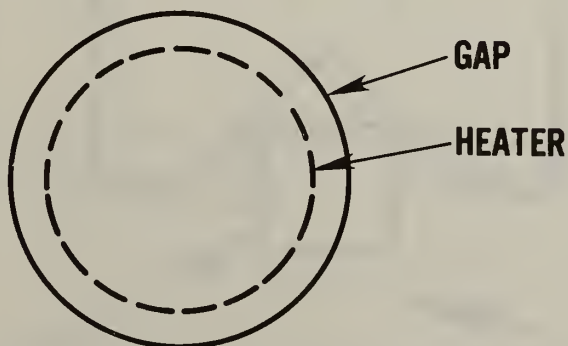
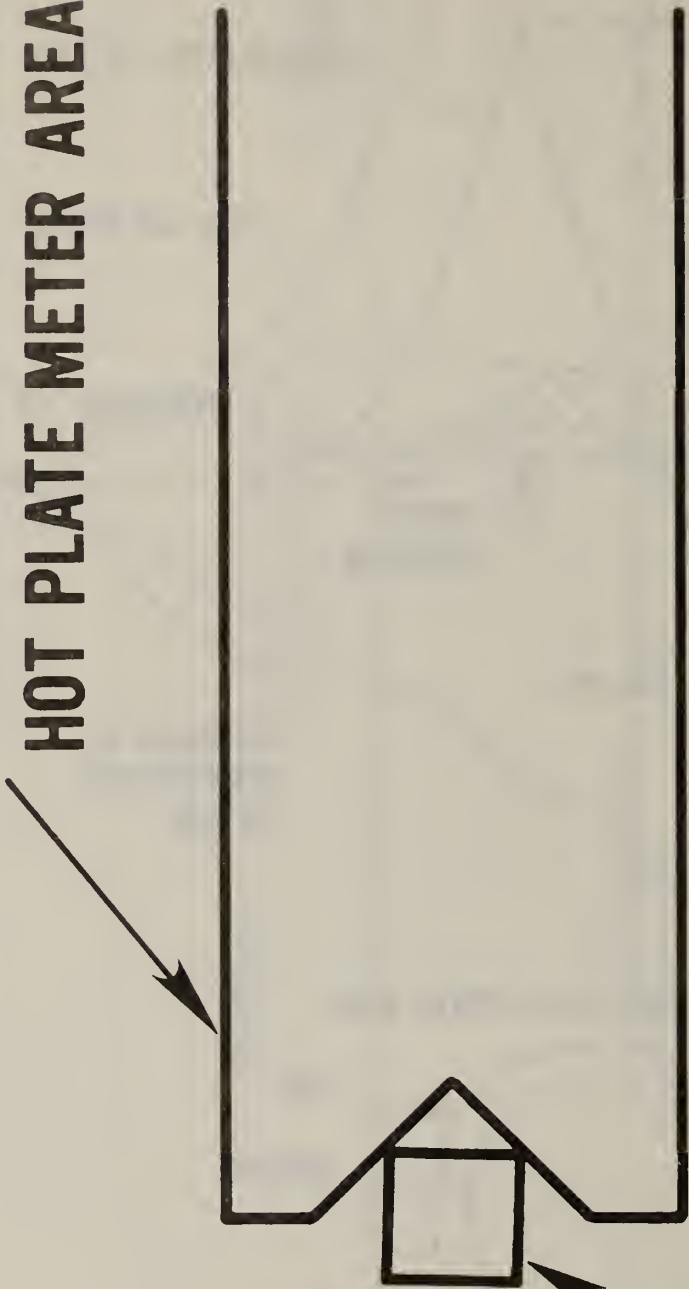


FIGURE 13 MEASURED HOT-PLATE, METER-AREA RADIAL TEMPERATURE DISTRIBUTION

**TEMPERATURE AT SURFACE OF  
HOT PLATE METER AREA**



**GAP**

**PLATINUM RESISTANCE  
THERMOMETER (PRT)**

FIGURE 14 FIGURE SHOWING TEMPERATURE  
UNCERTAINTY DUE TO HOT PLATE  
PRT LOCATION

U.S. DEPT. OF COMM. <b>BIBLIOGRAPHIC DATA SHEET</b> <i>(See instructions)</i>	<b>1. PUBLICATION OR REPORT NO.</b> NBSIR 83-2674	<b>2. Performing Organ. Report No.</b>	<b>3. Publication Date</b> April 1983
<b>4. TITLE AND SUBTITLE</b> ERROR ANALYSIS FOR THE NATIONAL BUREAU OF STANDARDS 1016 mm GUARDED HOT PLATE			
<b>5. AUTHOR(S)</b> Brian Rennex			
<b>6. PERFORMING ORGANIZATION</b> <i>(If joint or other than NBS, see instructions)</i> NATIONAL BUREAU OF STANDARDS DEPARTMENT OF COMMERCE WASHINGTON, D.C. 20234		<b>7. Contract/Grant No.</b>	<b>8. Type of Report &amp; Period Covered</b>
<b>9. SPONSORING ORGANIZATION NAME AND COMPLETE ADDRESS</b> <i>(Street, City, State, ZIP)</i> Department of Energy National Bureau of Standards			
<b>10. SUPPLEMENTARY NOTES</b>  <input type="checkbox"/> Document describes a computer program; SF-185, FIPS Software Summary, is attached.			
<b>11. ABSTRACT</b> <i>(A 200-word or less factual summary of most significant information. If document includes a significant bibliography or literature survey, mention it here)</i>  An error analysis is given for the 1-meter Guarded Hot Plate at the National Bureau of Standards. This apparatus is used to measure the thermal resistance of insulation materials. The individual contributions to uncertainty in thermal resistance are discussed in detail. The total uncertainty is estimated to be less than 0.5 percent at sample thicknesses up to 150 mm (6 inches) and less than 1 percent at a thickness of 300 mm (12 inches).			
<b>12. KEY WORDS</b> <i>(Six to twelve entries; alphabetical order; capitalize only proper names; and separate key words by semicolons)</i> Apparent thermal conductivity; error analysis; guarded hot plate; thermal insulation; thermal resistance.			
<b>13. AVAILABILITY</b> <input checked="" type="checkbox"/> Unlimited <input type="checkbox"/> For Official Distribution. Do Not Release to NTIS <input type="checkbox"/> Order From Superintendent of Documents, U.S. Government Printing Office, Washington, D.C. 20402.  <input checked="" type="checkbox"/> Order From National Technical Information Service (NTIS), Springfield, VA. 22161		<b>14. NO. OF PRINTED PAGES</b> 47	<b>15. Price</b> \$8.50





